Universitetet i Stavanger

FACULTY OF SCIENCE AND TECHNOLOGY

MASTER'S THESIS

Study program/specialization: Master of Science in Petroleum Engineering/ Natural Gas Technology	Spring semester, 2020. Open access
Author: Ofei Michael	_____ (Author's signature)
Supervisor(s): Dmitry Shogin	
Title of master's thesis: **Advanced modelling material functions of the Phan-Thein-Tanner (PTT) and Large amplitude oscillation shear (LAOS) flow modules**	
Credits: 30 ECTS	
Keywords: **Polymer** **Material function** **Shear stress start-up** **Shear stress relaxation** **Phan-Thien-Tanner models (PTT)** **Large amplitude oscillation shear flow (LAOS)**	Number of pages: + supplemental material/other: Stavanger, 15th July 2020

Abstract

The material functions of the linear and exponential Phan-Thein-Tanner (PTT) and Large amplitude oscillation shear (LAOS) modules are analyzed. The behaviour of the functions at inception and cessation are investigated using advanced mathematical modelling techniques. Starting with the affine PTT model expressions, they are further formulated using material function parameters for the steady, initiation and cessation shear flows. Dimensionless variables are introduced and incorporated into the equations and further modelling using Wolfram Mathematica is done to produce analytical results.
Further on, the formulations of the linear and exponential large amplitude oscillation shear (LAOS) modules are considered. They are also formulated using dimensionless variables and material functions. With the aid of Mathematica the equations are coded and plotted for a comprehensive analytical understanding of the behaviour of the flow. Ewoldt grid is introduced to give a better understanding of the Deborah De and Weissenberg Wi numbers effect as they increase or decrease on the behaviour of the flow.
The results gives a detail description of the behaviour of these modules under specific conditions and can be used with further studies in various fields.

Acknowledgement

To the Most High God, only wise and true be praise for leading me thus far and even amid the Covid-19 pandemic helping to survive and produce this work.

To the associate professor Dmitry Shogin who has been my constant inspiration and mentor even before and through out the writing of the thesis I express my highest gratitude. Never an email went unanswered and despite the challenges of social distancing always held online video calls to keep me in-tune. Assisting me in learning things I have never thought I could comprehend , and especially with the coding in Mathematica. Thank you Professor!!!

Special thanks to friends and family from the Stavanger Adventist Church for the moral, physical and spiritual support throughout my stay in Stavanger. Especially to Daniella, the Fira's, the Ommundsen's, Joeli and Sonja, the Claude's, the Ihebuzor's , Kenneth and Annemay, Kofi and Refan, Jonathan, my twin sister Jessica Meadows, and our pastors Damiono and May Anetta and all others I could not mention here.

Also, I would like to thank the Ghanaian community in Stavanger especially Mr Kwadwo-Atta Owusu and Maa Gina for their constant support and advice during this whole course of study.

To all my classmates from the University of Stavanger I am very thankful for the patience, help and the good times we shared together during this unique stage in my life. My friend Hardeejah(future professor), thank you for explaining difficult theories in a simple way.

To my former housemates at Madlastoken, I say thank you for your constant help and support at all times during the studies and throughout my stay here.

To all my colleagues and managers from Sumo Toll Hall restaurant, Radisson Blue Hotel and Foodora Riders Inc. am much grateful for your understanding and support in helping me balance my work-life with my studies and giving me the means to support my stay in Stavanger these years.

Last but not least , to my family; a firm bulwark unfailing, I express my heartfelt gratitude for your constant support and prayers. For believing in me when I have no reason to believe in myself. To my Mum and Dad, Sam, Law, Jemima and little Dora. Love you very much and may God richly bless the fruit of your labour...

Contents

List of Figures

List of Tables

Nomenclature

- normal Latin fonts for Scalar
- bold Latin fonts for Vector
- boldface Greek letters for Tensor notation

α cone angle

γ strain amplitude (%) for SAOS flow

$\dot{\gamma}$ shear rate

$\dot{\gamma}$ amplitude of shear rate oscillation (SAOS flow)

$\dot{\boldsymbol{\gamma}}$ rate of stress tensor

$\dot{\gamma_0}$ shear rate at time $t < 0$ for start-up and relaxation

δ unit tensor (Kronecker delta)

δ phase shift angle between present and resulting curve

ε permittivity of solvent

ε_0 permittivity of vacuum

$\eta(\dot{\gamma})$ shear stress dependence viscosity

$\psi_1(\dot{\gamma})$ first normal stress coefficient

$\psi_2(\dot{\gamma})$ second normal stress coefficient

η^* complex viscosity

$\eta^{'}$, $\eta^{''}$ complex viscosity coefficients

λ time constant

μ Newtonian fluid viscosity

π total stress tensor

ρ fluid density

$\boldsymbol{\tau}$ anisotropic stress tensor

$\tau_x x$ normal stress to X direction

$\tau_x y$ normal shear stress

$\tau_y y$ normal stress to Y direction

$\tau_z z$ normal stress to Z direction

$\Psi_1(\dot{\gamma})$ first normal stress coefficient

$\Psi_2(\dot{\gamma})$ second normal stress coefficient

ω frequency

c desired concentration of the diluted solution

c_0 true concentration of the mother solution

$c_s s$ conversion factor between M and τ

$c_s r$ conversion factor between n and $\dot{\gamma}$

$\boldsymbol{F}$ spring force

H spring stiffness

$\boldsymbol{g}$ gravitational force

$\mathbf{G}^{'}$ storage modulus

$\mathbf{G}^{''}$ loss modulus

k Boltzmann's constant

m consistency index (section 2)

m desired mass of the diluted solution (section 3)

M_c theoretical mass of the concentrated polymer

M_p required polymer

M_s measured mass of polymer solvent

$\boldsymbol{n}$ normal unit vector

n Power-law index (section 2)

n rotation per minute (section 3)

P thermodynamic pressure

$\mathbf{Q}$ vector between beads

Q extension of the spring

Q_0 maximum extension of the spring

q effective charge

S surface area

T temperature

t time

$\boldsymbol{v}$ fluid velocity

V volume item [Z] Z-factor

∇ vector differential operator

1. Introduction

Energy has and always will be an integral part of our lives; from lighting our homes to moving our cars and producing food for sustenance we cannot undermine the role energy plays in our daily lives. With the increase in population around the world and the limited resources we have to deal with, there is a challenge to keep up with the demands which awaits the world in the future. This means we have to find more efficient and sustainable ways to generate and use our energy [Nersesian 2014]. Oil and gas has been a reliable source of energy for the past years; serving as the anchor for various sectors in the economy and providing jobs for the masses.

Though some may argue that oil and gas is not a very sustainable resource, the fact that it will be in use for the coming years is inevitable. With new and diverse ways to generate energy been studied (*including wind, hydro, solar energies*), the petroleum industry cannot be deliberately ignored. Moreover, natural gas can be argued to be a more sustainable resource than its contemporary oil and devising ways to enhance its recovery is a subject matter of intense interest [Jin-gang 2004].

A general understanding of the kinetics of fluids then becomes essential, fluids behave differently when been transported through various mediums (pipes). The frictional resistance to flow through a pipe needs to be subdued by energy in the form of pressure. This resistance to flow is termed as *shear stress*, and the deformation it invokes on the fluid is called the *shear rate*. For most common fluids, like water, alcohol, air, etc the relationship between them are linear when plotted and this relationship is termed as *viscosity*. A fluid is therefore less viscous if the slope between the shear rate and shear stress is a low slope whiles it is more viscous when the slope is a high one [Ramsey 2019]. Figure [1] throws more light on this concept.

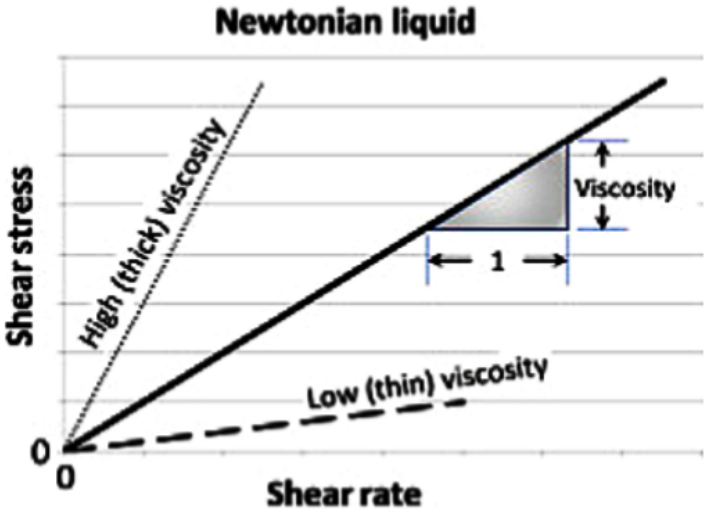

Figure 1: Newtonian fluid

.[Ramsey 2019]

Fluids that have a constant viscosity mathematically are defined as *Newtonian fluids* named after the renowned scientist Isaac Newton who discovered it. Generally , all fluids composed of small molecules are considered Newtonian. Examples of Newtonian fluids are water, brine, etc. In Newtonian fluids, the viscosity is not affected by the shear rate and they are easy to model and predict pressure behaviour. Non-Newtonian fluids on the contrary are fluids were a change in shear rate or pressure affects the viscosity; examples being polymers, gels, shampoo etc. Polymeric fluids in particular are used in many drilling activities. The terms polymeric fluids and non-Newtonian fluids are used interchangeable in this work.[Ramsey 2019]

In this research, we look at the properties of non-Newtonian fluids (polymers) and their use as a method to enhance oil recovery to facilitate optimal production from the reserves at our disposal. The process of injecting polymeric solutions to the reservoir to increase production is termed as *polymer flooding*. This method has been in use for a while with China and other countries tapping into the benefits it bestows. It is marked as one of the promising enhanced oil recovery (EOR) methods by the Norwegian Petroleum Directorate (NPD)[*Enhance oil recovery methods* n.d.] and hence getting a deeper understanding of the properties and behaviour of polymers is indispensable [Retorting 1978].

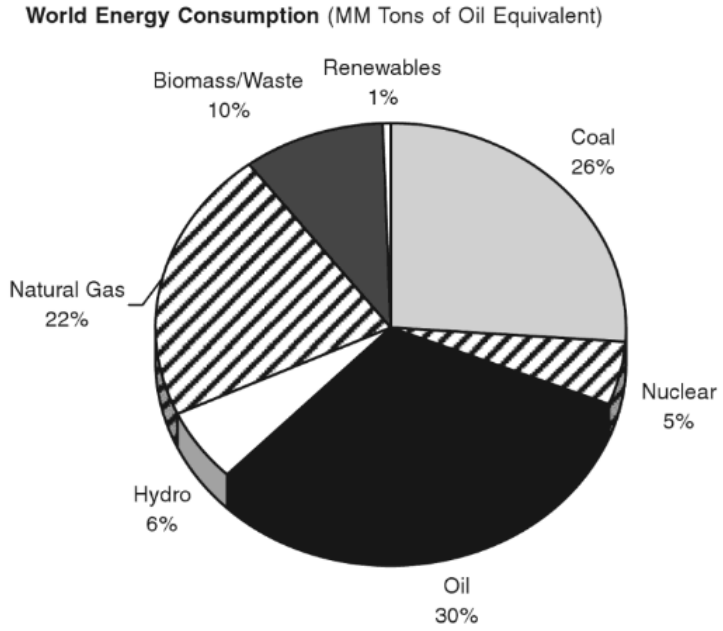

Figure 2: Statistics of Energy Consumption Worldwide.
[Retorting 1978]

1–1. Introduction to polymers

1–1.1. Versatility of polymers

The use of polymers transcend a wide variety of industries including but not limited to the aerospace industry, 3D printing, bio-polymers in molecular recognition, organic polymers in water purification, renewable energy industry *(wind,solar and biomass)*, making fireproof vest and fire-resistance jackets etc. Polymers are utilized in most solar innovations specifically in producing adhesives, coatings, moisture blockages, thermal and electrical insulation. They are also used as optical components in solar energy systems [*The Many applications of polymers* n.d.]. In the sphere of wind energy, they are used in making wind blades which maximize the lifespan and makes it resistance proof against corrosion and divers weather conditions.

Improved corrosive properties of polymers have been widely studied and confirmed. They are used widely due to their adhesive strength, high resistance to hazardous chemicals and their unique protective properties. This is largely due to the structure of the molecules which form polymers [Toorani and Aliofkhazraei 2019].

In the oil and gas industry the subject matter of EOR(Enhance Oil Recovery) methods bring to mind the two most used forms of water and polymer flooding which when implemented alternatively or together has proven to increase the oil recovery remarkably.

Figure 3: Estimated usage of polymer duplex coatings in various industries . [Toorani and Aliofkhazraei 2019]

1–1.2. Polymer Flooding

To increase oil recovery, different and diverse EOR methods are implemented to produce more oil at affordable prices. Among the different methods polymer flooding has proven to be very attractive for many reservoirs. Polymer flooding aims to control water mobility inside the reservoir to facilitate high recovery factors. It is one of the most promising EOR processes in many reservoirs with a low capital investment. To ensure favourable oil displacement, polymers are deployed to minimize mobility ratio between oil and water. Viscosity of the water being injected is enhanced by adding polymers which increase the area vertical sweep efficiency which boosts the oil recovery factor overall.

The technique of flooding with polymer has been in use for over 30 years with eventual recovery for over 50 percent. There are several factors that affect the outcome of polymer flooding such as the inaccessible pore volume, resistance factor and screen factor. Furthermore the performance of polymers are also a function of the polymer concentration. There are lower and upper limiting boundaries which render the results of polymer flooding ineffective [Algharaib, Alajmi, and Gharbi 2014].

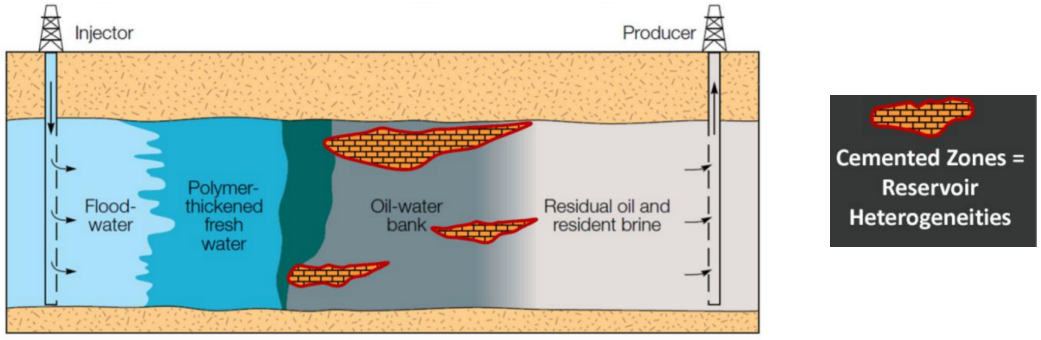

Figure 4: Polymer flooding reduce oil bypassing due to reservoir heterogeneities [Valencia, James, and Azmy 2015]

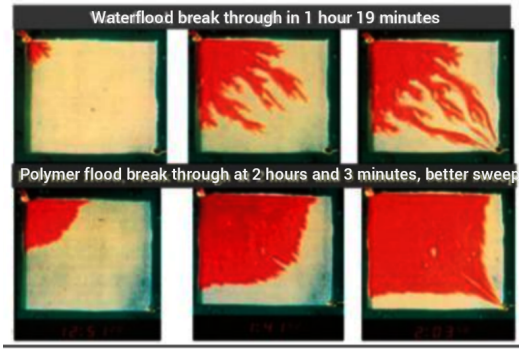

Figure 5: Sweep efficiency of water compared with polymer flooding [Valencia, James, and Azmy 2015]

With about 33% of oil-in-place which can be recovered by conventional methods, it is essential to implement polymer flooding to increase the sweep efficiency as seen in figure [5]. The challenges which comes with polymer flooding are the high temperatures and salinity effects of the water in the formation; these can to a large degree alter the properties of the polymer solution and hence its performance in oil recovery factor. There are developments underway to stabilize polymers under high temperatures and salinity environments but there has been no actual application yet.

1–1.3. Etymology of Polymers

The origins of polymers dates back to the beginnings of life in it's natural forms with polysaccharides, RNA and DNA being conspicuous in plant and animal life. Naturally occurring polymers have been capitalized on in making materials for varying needs including clothing, decoration, weapons, tools, shelter etc. The current industry of polymers though date back to the nineteenth century when vital discoveries came up with modifications of certain naturally occurring polymers [Young and Lovell 2011].

The science of polymers has undergone a wide range of studies and input by various researchers and scientist from its natural types to synthetic forms and their studies have been of immense interest to the scientific community ; spiking out varying debates about their properties, molecular structure and general applications.

What are Polymers?

A *Polymer* can be defined as a substance with molecules composed of group of atoms which are linked together by bonds *(covalent bonds mostly)*. Monomer molecules coming together through chemical reaction produces polymers , the process is termed as *polymerization*. Monomer molecules are molecules that can be bonded together to other similar molecules to form a polymer. The unique properties of polymers are mostly due to the fact that the molecules are long-chain linked to each other [Young and Lovell 2011].

The skeletal structure of polymers are represented as linear, cyclic, branched and networked. Linear polymers have a chain with two ends while the cyclic or ring polymers have no chain ends giving it peculiar properties from the former. Branched polymers have side chains and the networked polymers are interconnected with joints.

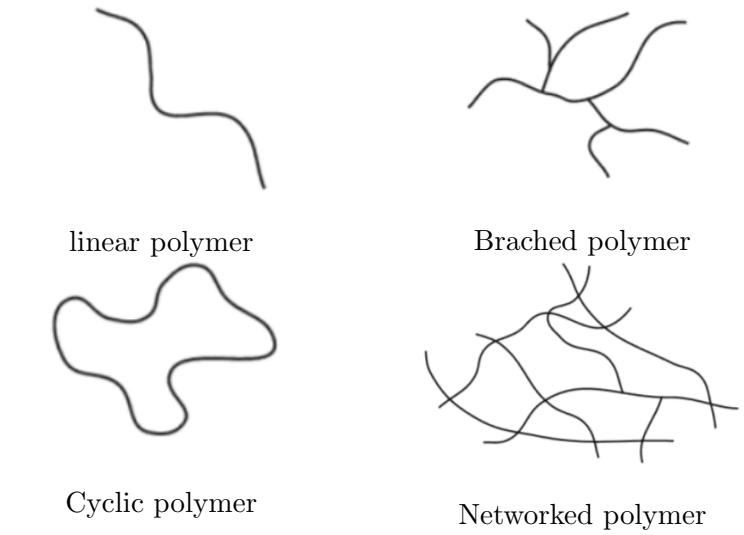

Figure 6: Skeletal structural representation of polymers

1–1.4. Viscosity of non-Newtonian fluids

One unflinching property of polymers that set them apart is the fact that they are dependant on the shear rate or non-Newtonian viscosity. This property can be well explain by an experiment where two identical vertical tubes with covered bottoms are filled with Newtonian and non-Newtonian fluids respectively. The Fluids are chosen so as to get the same viscosity in the experiment where the shear rate is low.

When a small sphere is put in them they drop at the same rates, which means the viscosity is the same in both the fluids. But when uncovered at the bottom the Newtonian fluid drains faster than polymeric fluid. It will be noticed that polymeric fluid exhibits a big shear rate when the bottom is uncovered than when the sphere is dropped in. This phenomena is referred to as *Shear thinning*. Viscosity in polymers under shear thinning can decrease by a factor of 10^3 or 10^4 [Robert Byron Bird, Armstrong, and Hassager 1987]

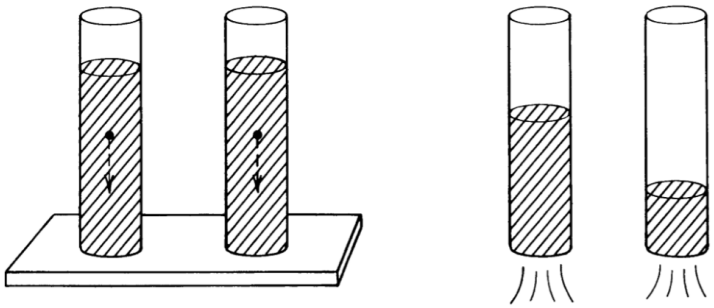

Figure 7: Shear thinning

.[Robert Byron Bird, Armstrong, and Hassager 1987]

There are however few non-Newtonian fluids that behave otherwise in this respect. These types flow at a lower pace than the Newtonian fluid when compared. This phenomena where fluids have an increasing viscosity with respect to shear rate is termed as *shear thickening* or *dilatant*. Other materials won't flow unless a certain yield stress is applied . Under this category falls paints , emulsifiers and greases [Robert Byron Bird, Armstrong, and Hassager 1987].

1–1.5. Effects of normal stress

The effects in the flow of polymeric fluids is largely affected by normal stress differences in shear flow. A way to better comprehend this is to label the differences in the normal stresses. If the fluid moves along the one coordinate alone and the speed varies in another direction then the direction is referred to as '1' direction ($\tau_{11} - \tau_{22}$), i.e., first normal stress. If it moves in the direction of velocity change is '2' direction ($\tau_{11} - \tau_{22}$), i.e., second normal stress and the remaining neutral direction, i.e., the '3' direction where speed is zero.

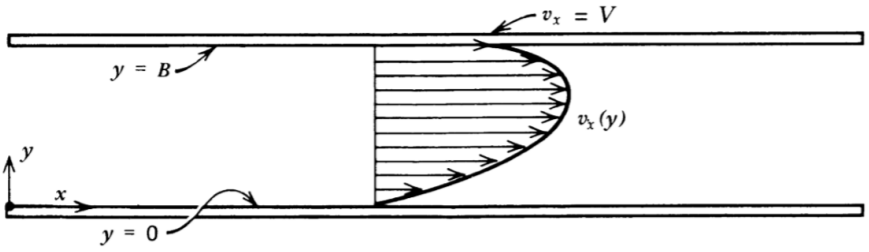

Figure 8: Flow between two plates with the upper plate moving
. [Robert Byron Bird, Armstrong, and Hassager 1987]

In *Figure 8* ; X and Y corresponds to 1 and 2 respectively. Polymeric fluids *first normal stress* difference appears to be practically negative and numerically greater than the *second normal stress* difference. This implies that polymeric fluids also have additional tension along streamlines or close to the sides which is proven by the Weissenberg's effect.

Experimental behaviour of non-Newtonian fluids

There are different experiments which explain the behaviour of non-Newtonian fluids, few are considered below to enlighten our understanding of how normal stress behaves;

- **Rod climbing :** In this experiment two beakers one containing a Newtonian and the other a non-Newtonian fluid are being rotated with rods at the same speed. It is noted that in the Newtonian fluid it is pushed downwards due to centrifugal forces causing a dip in the center. On

the other hand, the polymer solution exhibits an opposite effect where the fluid climbs towards the center of the rod. And the results can be more striking at higher speeds.

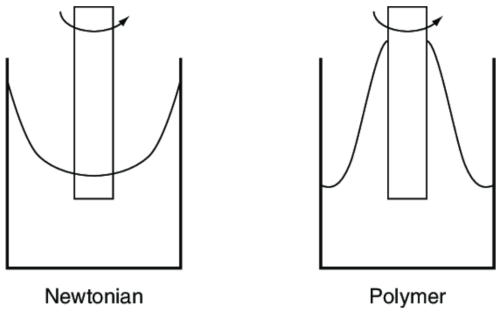

Figure 9: Rod-climbing effect

.

- **Magnet stirrer :** With this experiment two beakers are filled one with non-Newtonian and the other Newtonian fluid and placed on a magnetic stirrer. The set-up is put to motion at the same speed and it is noticed that the non-Newtonian fluid forms tornado-like vortex with a dip inside forming from the center of the magnet. On the contrary , the polymer solution forms a cone-shaped on the surface.

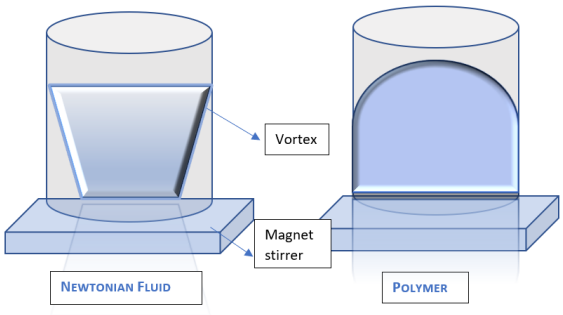

Figure 10: Fluid behaviour with a magnetic stirrer

.

- **Die swell effect:** In the die swell or extrudate experiment fluids of non-polymeric and polymeric exits from capillaries respectively with a given diameter of say D. The diameter it attains as it flows out of the capillary then becomes D_f. It is noticed that the diameter of the fluid as it comes out of the Newtonian fluid remains practically the same whiles the polymeric fluid attains an increase of about 300%. An extrudate diameter of two to four times the diameter of the capillary , this is known as *extrudate swell*.

Extrudate swell can be attributed to a number of factors ; it can be explained by the effect of normal stresses at the end of the capillary. Moreover , the polymer molecules near the tube wall undergo stretching than those in the center thus the bouncing back the molecules close to the liquid-gas interface contributing to the swelling. There is however no one simple analysis of this very complicated phenomena.

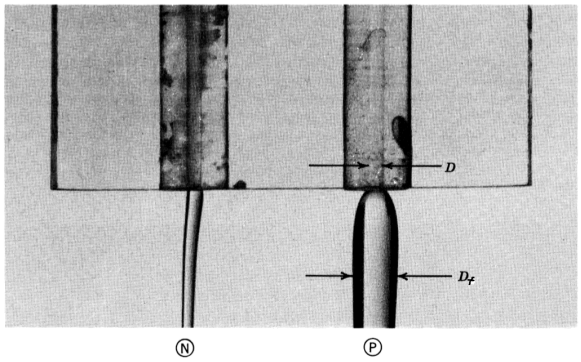

Figure 11: Fluid behaviour from capillary tube
. [Robert Byron Bird, Armstrong, and Hassager 1987]

2. Review of fluid dynamics

2–1. Fluid dynamics

The dynamics of fluids are rightly represented by equations that describe how such fluids flow. These equations, also known as the 'equations of change' show how the mass, momentum and energy exhibited by the fluids transform with respect to time and space [Robert Byron Bird, Armstrong, and Hassager 1987].
To validate the representation of any type of fluid , different notations are used. Also, it is paramount to have an overall understanding of the velocity field of a fluid. Hence the equations of conservation of mass and momentum will have to be ascertain.

Mathematical notations

In the studies of polymeric fluids the physical quantities generally employed to assist in calculations are classified into tensors, scalars and vectors.
Tensors (rank two) are physical quantities which assign a number to an ordered pair of vectors. Their coordinate representation, which is a matrix depends on the frame of reference. They are objects which define the relation between algebraic objects related to vector space. Examples include stress, rate of strain, etc.
Scalars are physical quantities that can be expressed as a single element of a number field (real number) usually coming with with a unit. Can also be termed as a tensor of zero rank. Examples are shear rate, temperature, volume.
Vectors are physical quantities that have a magnitude and direction. They are also tensors of first rank. Example of vectors are momentum, force and velocity.
To have clear distinction between them the following notations are being used in this research work.

- Normal Latin fonts for scalar notation
- Bold face Greek letter for Tensor notation
- Boldface Latin fonts for vector notation

2–1.1. Mass conservation

The concept of mass conservation expounds the fact that if the mass flowing into a system is not equal to the mass flowing out of the system, then there will be a change in the volume or density in the volume of consideration. This principle as other laws in physics is pragmatic; which implies it is based on experimental results.

Assuming that the element of volume $\boldsymbol{v}$ with a surface area S has a small surface element d with a velocity $\boldsymbol{v}$. The volume rate of flow across d will be;

$$(\boldsymbol{n} \cdot \boldsymbol{v})\mathrm{d}S. \tag{2.1}$$

For an outward flow $(\boldsymbol{n}\cdot\boldsymbol{v})\mathrm{d}S$ tends to be positive whiles for an inward flow $(\boldsymbol{n}\cdot\boldsymbol{v})\mathrm{d}S$ becomes negative. The mass rate of flow is then given by $(\boldsymbol{n} \cdot \rho\boldsymbol{v})\mathrm{d}S$. Where $\rho\boldsymbol{v}$ represents the mass per unit area per unit time [Robert Byron Bird, Armstrong, and Hassager 1987].

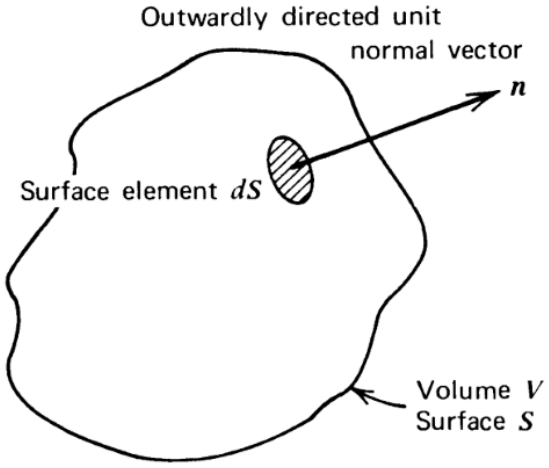

Figure 12: Fixed volume over which the balances of mass,momentum and energy are written [Robert Byron Bird, Armstrong, and Hassager 1987]

.

Regarding mass conservation, the entire mass of fluid in V will only change due to a net influx of fluid which moves across the main surface S.

$$\frac{\mathrm{d}}{\mathrm{d}t}\int_V \rho \mathrm{d}V = -\int_s (\boldsymbol{n} \cdot \rho\boldsymbol{v})\mathrm{d}S. \tag{2.2}$$

Introducing Gauss's divergence theorem, the surface integral is transformed into a volume integral,

$$\frac{\mathrm{d}}{\mathrm{d}t}\int_V \rho \mathrm{d}V = -\int_V (\nabla \cdot \rho\boldsymbol{v})\mathrm{d}V \tag{2.3}$$

When the equation is rearranged with the introduction of time derivative it becomes;

$$\int_V \left[\frac{\partial \rho}{\partial t} + (\nabla \cdot \rho\boldsymbol{v})\right] \mathrm{d}V = 0 \tag{2.4}$$

$$\frac{\partial \rho}{\partial t} = -(\nabla \cdot \rho\boldsymbol{v}). \tag{2.5}$$

With a constant density the equation of continuity simplifies to

$$(\nabla \cdot \upsilon) = 0. \tag{2.6}$$

2–1.2. Momentum conservation

The principle of momentum conservation is derived from Newton's second law of motion which states that acceleration of a body is proportional to the net force acting on it and inversely proportional to its mass.

$$\text{Acceleration (a)} = \frac{\text{Force}(\mathbf{F})}{\text{mass(m)}}. \tag{2.7}$$

The linear momentum is define as the product of the mass and acceleration ie;

$$\text{Momentum} = \text{mass(m)} \times \text{acceleration(a)}.$$

Hence the rate of change in speed of a body equals the momentum of the body. Considering the initial example from section [2–1.1], momentum conservation equation can be ascertained when $(\boldsymbol{n} \cdot \boldsymbol{v})\mathrm{d}S$ is multiplied to the per unit volume of the fluid's momentum giving as a product of $(\boldsymbol{n} \cdot \boldsymbol{v})\rho\boldsymbol{v}\mathrm{d}S$.
Simplified it becomes $n \cdot \rho\boldsymbol{v}\boldsymbol{v}\mathrm{d}S$, with $\rho\boldsymbol{v}\boldsymbol{v}$ signifying the momentum flux associated with the whole flow of the fluid.
Moreover the momentum transfer by virtue of the interactions within the fluid and molecular motions is represented by $\boldsymbol{\pi}$, which is a second order tensor. The rate of change momentum flow coming about by molecular interactions then becomes

$$\boldsymbol{n} \cdot \boldsymbol{\pi}\mathrm{d}S.$$

The law of momentum conservation then becomes

$$\frac{\mathrm{d}}{\mathrm{d}t}\int_v \rho\mathbf{v}\mathrm{d}V = -\int_s [\mathbf{n} \cdot \rho\boldsymbol{v}\boldsymbol{v}]\mathrm{d}S - \int_s [\mathbf{n} \cdot \boldsymbol{\pi}]\mathrm{d}S + \int_v \rho\mathbf{g}\mathrm{d}V. \tag{2.8}$$

Where g here represents the force per unit mass with respect to gravity. Simplifying further with Gauss theorem and forgoing the integral signs it becomes:

$$\frac{\partial}{\partial t}\rho\boldsymbol{v} = -[\boldsymbol{\nabla} \cdot \rho\boldsymbol{v}\boldsymbol{v}] - [\boldsymbol{\nabla} \cdot \boldsymbol{\pi}] + \rho\mathbf{g}. \tag{2.9}$$

Equation [2.8] is referred to as the equation of motion. The tensor $\boldsymbol{\pi}$ exhibits alternate interpretation where the surface force term in equation [2.9] could have the form -$\int$ $\boldsymbol{\pi_n}$ dS, with $\boldsymbol{\pi_n}$ dS representing a vector which describes the force exerted by the fluid's positive and negative sides of dS. Comparing the above integral with the term in [2.8] the conclusion is drawn that $\boldsymbol{\pi} = [\boldsymbol{n} \cdot \boldsymbol{\pi}]$.

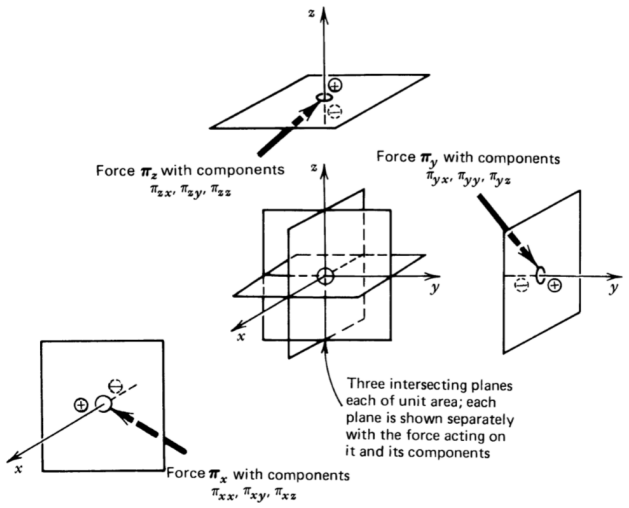

Figure 13: Interpretation of the diagonal components of the stress tensor as normal forces [Robert Byron Bird, Armstrong, and Hassager 1987].

This implies that the force $\pi \mathrm{d}S$ corresponding to any orientation $\mathbf{n}$ of $\mathrm{d}S$ can be ascertained from the tensor π. The force acting on the positive j-direction and perpendicular to i- direction can be rightfully represented by π_{ij}.

Expounding on equation [2.9] using dot product of velocity vector υ, equation of motion and equation of continuity, these equations are ascertained for kinetic and angular momentum

$$\frac{\partial}{\partial t}\left(\frac{1}{2}\rho\upsilon^2\right) = -\left(\boldsymbol{\nabla}\cdot\frac{1}{2}\rho\upsilon^2\boldsymbol{\upsilon}\right) - (\boldsymbol{\upsilon}\cdot[\boldsymbol{\nabla}\cdot\boldsymbol{\pi}]) + \rho(\boldsymbol{\upsilon}\cdot\boldsymbol{g}) \tag{2.10}$$

$$\frac{\partial}{\partial t}(\rho[\boldsymbol{r}*\boldsymbol{\upsilon}]) = -[\boldsymbol{\nabla}\cdot\rho\boldsymbol{\upsilon}[\boldsymbol{r}*\boldsymbol{\upsilon}]] - [\boldsymbol{\nabla}\cdot[\boldsymbol{r}*\boldsymbol{\pi}]^{\dagger}] + [\boldsymbol{r}*\boldsymbol{\rho g}]. \tag{2.11}$$

The symbol † represents the transpose tensor. The last but not least is the third law which won't be explored here.This is the energy conservation law which is used in the calculation of non-isothermal equations.

2–2. Material functions of polymeric fluids

Newton's law of viscosity alone is not sufficient for describing macro-molecular fluids , their properties (of non-Newtonian fluids) plays a major role in defining them.

This brings us up the subject matter of material functions of non-Newtonian fluids. Material functions are functions composed of flow parameters namely time, shear rate, frequency, etc that characterize the rheological effects of fluids response(in terms of stresses) in a certain simple flow without reference to force or mass. To begin with, it is paramount to know the flow patterns of these fluids. The density ρ and viscosity μ can be termed in-compressible in Newtonian fluids at constant temperature but for

non-Newtonian fluids it can be more complicated. Experiments conducted on the polymers can yield a host of material functions that depend on frequency, shear rate, time and many more.
[Robert Byron Bird, Armstrong, and Hassager 1987]

2–2.1. Shear flow

The term *shear flow* is used to define a flow generated by a force in a fluid. Amid shear flow, a fluid flows at different speeds though adjacent and parallel, which can be due to a moving plate. Owning to the viscousness of the fluid there is a resistance which is manifested as stress. The stress is directly related to the shear rate in Newtonian fluids but Non-Newtonian fluids exhibit a different behaviour. A simple shear flow using Cartesian coordinates can be represented by the velocity fluid

$$v_x = \dot{\gamma}_{yx} y; \qquad v_y = 0; \qquad v_z = 0.$$

As represented in figure [2–2.1], where the velocity gradient $\dot{\gamma}_{yx}$ is a function of time with an absolute value called the shear rate $\dot{\gamma}$. Shear rate is independent of time and with the assumption that it has been constant for a long period of time, all stresses are considered time-independent.
It is a common type of flow in rheology. There is no mixture as the layers of flow pass each other, flow is rectilinear and velocity varies in just one direction. Particle path in simple shear flow are straight parallel lines.
[Robert Byron Bird, Armstrong, and Hassager 1987]

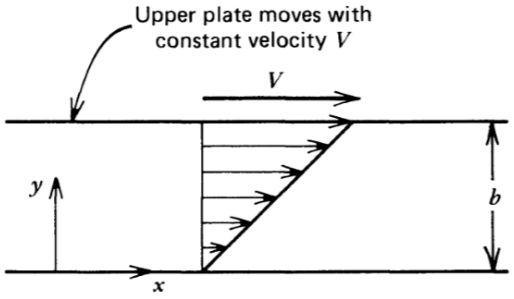

Figure 14: Simple shear flow
[Robert Byron Bird, Armstrong, and Hassager 1987].

Stress tensors for shear flow

For non-Newtonian fluids assumptions are made that in any flow the six independent components of the stress tensor is not zero. But in simple shearing flows of in-compressible fluids it can be shown that just three of the components are measurable at the most [Robert Byron Bird, Armstrong, and

Hassager 1987]. The form of the stress tensor for simple shearing flow becomes :

$$\boldsymbol{\pi} = p\boldsymbol{\delta} = +\boldsymbol{\tau} = \begin{pmatrix} p+\tau_{xx} & \tau_y x & 0 \\ \tau_{yx} & p+\tau_{yy} & 0 \\ 0 & 0 & p+\tau_{zz} \end{pmatrix} \tag{2.12}$$

For fluids that are in-compressible the normal stress and the pressure cannot be separated on surfaces and therefore the quantities of interest become the shear stress and two normal stress differences [Robert Byron Bird, Armstrong, and Hassager 1987]. Stresses associated with shear flow are as follows:

$$\text{Shear stress} : \tau_{yx} \tag{2.13}$$

$$\text{First normal stress difference} : \tau_{xx} - \tau_{yy} \tag{2.14}$$

$$\text{Second normal stress difference} : \tau_{yy} - \tau_{zz} \tag{2.15}$$

$$\tag{2.16}$$

2–2.2. Shearfree flow

In a simple shearfree flow the stresses are not time dependant, the elongation rate ($\dot{\varepsilon}$) is assumed to be a constant over a significant period of time and it is represented by the velocity field ;

$$\begin{aligned} \upsilon_x &= -\frac{1}{2}\dot{\varepsilon}(1+b)x \\ \upsilon_y &= -\frac{1}{2}\dot{\varepsilon}(1+b)y \\ \upsilon_z &= +\dot{\varepsilon}z. \end{aligned} \tag{2.17}$$

Where b is a numerical value $0 \leq b \leq 1$ and $\dot{\varepsilon}$ is the elongation rate which can depend on time. The types of shearfree flows which come about with varying values of b are:

$$\text{Elongational flow} : (b = 0, \dot{\varepsilon} > 0)$$

$$\text{Biaxial stretching flow} : (b = 0, \dot{\varepsilon} < 0)$$

$$\text{Planar elongational flow} : (b = 1)$$

The value of b has a rippling effect on the structure of the streamlines rotation around the z-axis. Steady shearfree flow implies that $\dot{\varepsilon}$ is not dependent on time [Robert Byron Bird, Armstrong, and Hassager 1987].

In many polymer operations shearfree flow is encountered; among them are shear stretching, fibre spinning, vacuum thermoforming etc. Flows that occur around corners, stagnation points and through contractions have an elongational character but are however considered not entirely shearfree flows because they occur around solid boundaries [Robert Byron Bird, Armstrong, and Hassager 1987].

Stress tensor for shear free flow

Shear free flow shows more symmetry than ordinary shear flow. With a rotation of 180° around *x-axis, y-axis, or z-axis* there is no deformation. The symmetry together with the fluid isotropy (*uniformity in all orientations*) for a stress free tensor is given by :

$$\boldsymbol{\pi} = p\boldsymbol{\delta} + \boldsymbol{\tau} = \begin{pmatrix} p+\tau_{xx} & 0 & 0 \\ 0 & p+\tau_{yy} & 0 \\ 0 & 0 & p+\tau_{zz} \end{pmatrix}. \tag{2.18}$$

For in-compressible fluids the only two normal stress difference with respect to experimental undertakings are:

$$\begin{aligned} &\tau_{zz} - \tau_{xx} \\ &\tau_{yy} - \tau_{xx}. \end{aligned} \tag{2.19}$$

As noted in section [2–2.2], b has a value of 0 for elongational and biaxial stretching flows, differentiating between x and y directions is not possible making $\tau_{xx} - \tau_{yy} = 0$ and leaving just one normal stress difference to be ascertained.

2–2.3. Material functions for steady shear flow

Steady-state stresses, if assumed to depend solely on the flow field can then be considered as functions only of shear rate $\dot{\gamma}$.

$$\tau_{xy} = -\eta(\dot{\gamma})\dot{\gamma}_{yx} \tag{2.20}$$

The coefficients of the normal stress Ψ_1 and Ψ_2 are defined as :

$$\begin{aligned} \tau_{xx} - \tau_{yy} &= -\Psi_1(\dot{\gamma})\dot{\gamma}_{yx}^2 \\ \tau_{yy} - \tau_{zz} &= -\Psi_2(\dot{\gamma})\dot{\gamma}_{yx}^2 \end{aligned} \tag{2.21}$$

Bearing in mind that, Ψ_1 and Ψ_2 represent the first and second normal stress coefficients respectively. The η, Ψ_1 and Ψ_2 are sometimes referred to as the viscometric functions. When there is a change in sign of $\dot{\gamma}_{yx}$ in Equation [2.20], it changes the shear stress sign also. On the other hand, the normal stress difference doesn't change sign if $\dot{\gamma}_{yx}$ changes sign in equations [2.21]. The viscosity is the best known function experimentally [Robert Byron Bird, Armstrong, and Hassager 1987].

When shear rates are at the minimum, their values are proportional to $\dot{\gamma}$, while the viscosity approaches a constant value known as the *zero-shear-rate viscosity*. When shear rates approach higher values the viscosity of most polymeric fluids decrease with increasing shear rate. This appears to be a very important characteristic of polymeric liquids in many engineering applications [Robert Byron Bird, Armstrong, and Hassager 1987].

When the viscosity is plotted against the shear rate using log graph it has a linear region when the shear rates are high which turns to remain constant over a decades of decreasing viscosity.

Experimentally this region is known as the *power-law region*. The power-law region can be somewhere between -0.4 to -0.9 for normal polymeric liquids. At higher shear rates the viscosity becomes independent of shear rate and approaches infinity this is termed as the *infinite-shear-rate viscosity*. The η for concentrated solutions is practically immeasurable since at high shear rates there is an issue with polymer degradation [Robert Byron Bird, Armstrong, and Hassager 1987].

For Newtonian fluids Ψ_1 and Ψ_2 are equivalent to 0. And when $\tau_{xx} - \tau_{yy}$ is negative and $\tau_{yy} - \tau_{zz}$ is positive they carry the meaning of an extra compression in the direction of y. Therefore to maintain steady shear flow a normal force is applied to the parallel plates to keep them together when dealing with polymeric fluids.

Shear stress is just necessary to keep steady shear flow for Newtonian fluid. Elasticity in the fluid is calculated by the the stress ratio, $(\tau_{xx} - \tau_{yy}/\tau_{yx})$. For Newtonian fluids, the value is 0 and is the same for non-Newtonian fluids with respect to small shear rates [Robert Byron Bird, Armstrong, and Hassager 1987].

2–2.4. Material functions for unsteady shear flow

Unsteady shear flow can be defined as a flow that is dependant simultaneously on frequency *(time)* and shear rate amid time-dependant shearing flow.

As is the case in steady shear flow, there are also three measurable quantities of the unsteady shear flow; these are the shear stress (η) and the two normal stress differences ($\mathbf{\Psi_1}, \mathbf{\Psi_2}$).

Different laboratory test are used in rheology for ascertaining the measurable stress properties, of which we will consider a few.

[Robert Byron Bird, Armstrong, and Hassager 1987]

2–2.5. Small Amplitude Oscillatory Shear (SAOS)

In this experiment, the response of an unsteady sample which is placed between two parallel plates is carefully scrutinized. During the experiment the upper plate is oscillated sinusoidally with a frequency of ω. The immediate speed profile will be close to linear in y if $\omega\rho h^2/2\eta_0 \ll 1$, with h being the distance between the upper and lower plates. The shear strain for a linear velocity profile between times 0 and

t is $\gamma_{yx}(0,t) = \int_0^t \dot{\gamma}_{yx}(t')\mathrm{d}t'$ [Robert Byron Bird, Armstrong, and Hassager 1987].
The Shear rate at time t not considering the position is given as :

$$\begin{aligned} \gamma_{xy}(0,t) &= \gamma^\circ \sin \omega t \\ \dot{\gamma}_{xy}(t) &= \gamma^\circ \cos \omega t = \dot{\gamma}^\circ \cos \omega t, \end{aligned} \tag{2.22}$$

γ° and $\dot{\gamma}^\circ$ here stands for the positive amplitudes of the shear strain and rate oscillations. Regarding polymeric fluids the shear stress oscillates with the ω and the normal stress with 2ω close to a nonzero mean value.
Amplitude and phase shift of the shear stress can be measured as a function of the frequency ω, the assumption made here is that the shear strain amplitude γ° is relatively small. The shear stress is linear with respect to the stain rate [Robert Byron Bird, Armstrong, and Hassager 1987];

$$\tau_{yx} = -A(\omega)\gamma^\circ \sin(\omega t + \delta) \qquad (0 \leq \delta \leq \pi/2) \tag{2.23}$$

$$\tau_{yx} = -B(\dot{\omega})\gamma^\circ \cos(\omega t - \mathbf{\Phi}) \qquad (0 \leq \mathbf{\Phi} \leq \pi/2) \tag{2.24}$$

In this equation $\mathbf{\Phi} = (\pi/2) - \delta$. If the equation is redefined with the in-phase and out of phase parts of the stress it takes the form:

$$\tau_{yx} = -G'(\omega)\gamma^\circ \sin\ \omega t - G''(\omega)\gamma^\circ \cos\ \omega t \tag{2.25}$$

$$\tau_{yx} = -\eta'(\omega)\gamma^\circ \cos\ \omega t - \eta''(\omega)\dot{\gamma}^\circ \sin\ \omega t \tag{2.26}$$

Further more it can be noticed that $G', G''$and $\eta', \eta''$are related to A, δ and $B, \mathbf{\Phi}$ respectively:

$$A(\omega) = \sqrt{G'^2 + G''^2} = |G^*|, \qquad \tan\delta = G''/G' \tag{2.27}$$

$$B(\omega) = \sqrt{\eta'^2 + \eta''^2} = |\eta^*|, \qquad \tan\delta = \eta''/\eta' \tag{2.28}$$

The symbols $|G^*|$ and $|\eta^*|$ represent the magnitudes of the complex modulus and the complex viscosity respectively.

These functions are important in the characterization of the behaviour of small deformations and are sometimes referred to as the *linear viscoelastic properties.* G$'$(*storage modulus*) gives an understanding about the elastic characteristics of the fluid in energy storage during a change is shape. On the contrary G$''$ gives information about the energy loss if flow and most times referred to as the *loss modulus.*
The dynamic viscosity is represented here by η' while the angle between the stress and stain is $\tan\delta$ also called the loss tangent.
[Robert Byron Bird, Armstrong, and Hassager 1987]

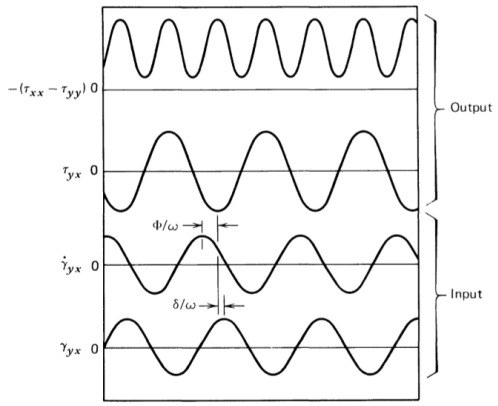

Figure 15: Oscillatory Shear Strain,Rate,Stress and First Normal Stress Difference in SAOS [Robert Byron Bird, Armstrong, and Hassager 1987]

2–2.6. Inception of steady shear flow

The initiation experiment begins with the assumption that the fluid is at rest for all times preceding $t = 0$. The velocity gradient is γ_0 for the times ≥ 0.

The subject matter of interest is the examination of the stresses as they approach their steady shear flow values. The functions $\eta^+(t, \dot{\gamma}_0), \mathbf{\Psi}_1^+(t, \dot{\gamma}_0),$ and $\mathbf{\Psi}_2^+(t, \dot{\gamma}_0)$ are redefined in light of $\eta, \mathbf{\Psi}_1$and $\mathbf{\Psi}_2$ respectively to define the normal stress differences and transient shear stress.

The steady shear rate is applied for positive times hence the plus superscript and these time dependant properties are measured in various instruments such as a cone and plate instrument. For larger shear rates the η^+ first attains a maximum and approaches a steady-state value after few oscillations, whiles at small shear rates the stresses approaches their steady-flow values unconditionally [Robert Byron Bird, Armstrong, and Hassager 1987].

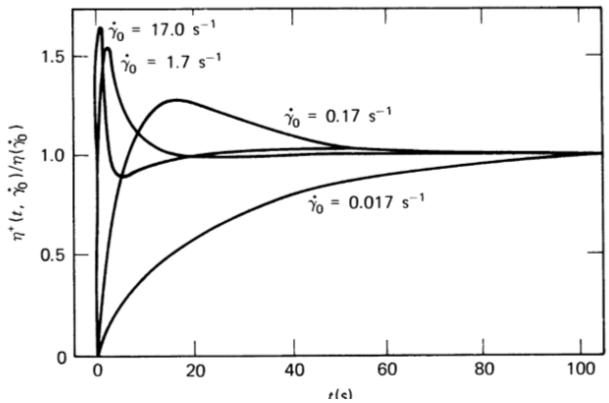

Figure 16: Shear stress growth function of 1.5 % polyacrylamide in a 50/50 mixture by weight of water and glycerin [Robert Byron Bird, Armstrong, and Hassager 1987]

2–2.7. Stress relaxation after cessation of steady Flow

This experiment considers the movement of a fluid going through steady shear flow with a shear rate $\dot{\gamma}_0$, which abruptly is stopped at a time $t = 0$ implying that $\dot{\gamma} = 0$ for $t \geq 0$.
The relaxing stresses are characterized by the material functions $\eta^-(t, \dot{\gamma}_0), \mathbf{\Psi}_1^-(t, \dot{\gamma}_0)\text{and}\mathbf{\Psi}_2^-(t, \dot{\gamma}_0)$ defined to the viscometric functions. The minus superscript here serves as a reminder that the steady shear flow occurred for negative times, the $\dot{\gamma}_0$ in every function is an indication of the dependence on the shear rate.
The end results of the experiment concludes that there is a constant convergence of the stresses to zero and they even relax faster as the preceding shear flow in increased. Shear stresses relax much faster that the first normal stress difference.
[Robert Byron Bird, Armstrong, and Hassager 1987]

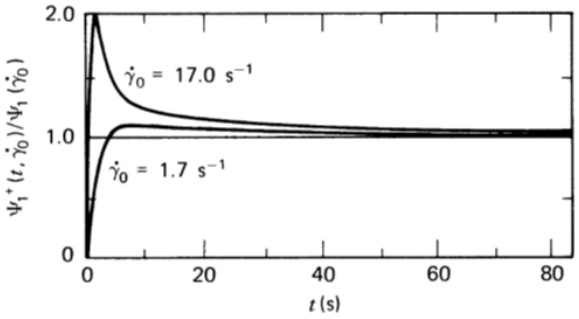

Figure 17: First normal stress growth function of 1.5 % polyacrylamide in a 50/50 mixture by weight of water and glycerin

Weissenberg and Deborah numbers

To quantify viscoelastic effects in fluid flow two dimensionless variables are used; namely the *Weissenberg* (Wi) and the *Deborah* (De) numbers. Although unique from each other in the effects they describe, they are used sometimes as synonyms;

- Weissenberg's Effect:

  Weissenberg's effect basically explains that there is extra tension along the stream lines when the polymer flows i.e. a force which acts normal to the streamlines. The Weissenberg effect is characterized by the Weissenberg number which relates the elastic forces to the viscous forces in a fluid and is represented by Wi. It is a dimensionless number which is a product of the shear rate ($\dot{\gamma}$) by the relaxation time (λ) [Poole 2012];

$$\mathrm{Wi} = \frac{\text{elastic forces}}{\text{viscous forces}} = \frac{\tau_{xx} - \tau_{yy}}{\tau_{xy}} = \frac{\lambda\mu\dot{\gamma}^2}{\mu\dot{\gamma}} = \dot{\gamma}\lambda. \tag{2.29}$$

- Deborah Number:

  The Deborah number was named after the prophetess Deborah in the Bible who said "*The mountain flowed before the Lord....*". It shows how of a material will act over a given period of time with the assumption that it deforms over this period [Poole 2012].

$$\mathrm{De} = \frac{\text{relaxation time of material}}{\text{deformation time}} = \frac{\lambda}{T} \tag{2.30}$$

It is expected to notice a fluid behavior in a material if the observation time is longer or it has a short relaxation time and inversely is true for a solids [Poole 2012].

2–2.8. Large amplitude oscillation shear (LAOS)

In rheological experiments, dynamic oscillatory tests methods are used to investigate the properties of polymers. As already discussed the small amplitude oscillatory shear (SAOS) tests are widely used to investigate the linear viscoelastic properties due to it's easy applicability and the many supporting research behind it.

But there are situations where the deformations can be large and increasingly fast and hence the non-linear material properties exert major control on the system's output. This then leads to an overall sample characterization which will factor in the non-linear properties been overlooked.

As a result large amplitude oscillatory shear test can be implemented to understand and quantify the nonlinear viscoelastic behavior of complex polymeric fluids which can be encountered when implementing polymer flooding [Hyun et al. 2011].

In this experiment the polymeric fluid is subjected to shear apparatus where it is confined and subjected to a boundary of solid-liquid to a co-planner sinusoidal displacement [Saengow, Alan Jeffrey Giacomin, and Kolitawong 2015].

The velocity profile of the fluid is described in figure [18];

$$\upsilon_x = \dot{\gamma}^0 \cos\omega t * y \tag{2.31}$$

where $\upsilon_y = \upsilon_z = 0$.

For a corresponding co-sinusoidal shear rate the expression becomes:

$$\dot{\gamma}(t) = \dot{\gamma}^0 \cos\omega t. \tag{2.32}$$

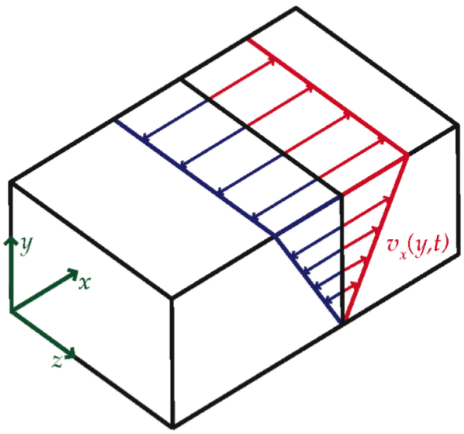

Figure 18: Orthomorphic isometric sketch of alternating velocity profile in oscillatory flow. [Saengow, Alan Jeffrey Giacomin, and Kolitawong 2015]

Equation [2.32] can be rewritten by the variable λ, while implementing the properties of cessation time of the viscoelastic fluid:

$$\lambda\dot{\gamma}(t) = \lambda\dot{\gamma}^0 \cos\lambda\omega(t/\lambda) \tag{2.33}$$

$$\equiv \mathrm{Wi}\cos\mathrm{De}(t/\lambda) \tag{2.34}$$

Where it can be observed that $\mathrm{De} \equiv \lambda\omega$ and $\mathrm{Wi} \equiv \lambda\dot{\gamma}^0$.
With the introduction of the dimensionless Equation [2.34], the dimensionless solutions to problems of large oscillatory nature can be presented in written terms of just the Wi and De.
Higher harmonics are seen in the shear stress response under Large amplitude oscillatory shear(LAOS). With polymeric fluids this happens when;

$$\mathrm{Wi}/\mathrm{De} > 1. \tag{2.35}$$

which becomes our working definition for large amplitude oscillatory shear flow. Experiments can be carried out with respect to Equation 2.35 due to much progress in rheometry. The material functions in this type of flow are often represented as coefficients of the Fourier series as in Equation [2.36] :

$$\frac{\boldsymbol{\tau_{yx}}(\boldsymbol{\tau},\gamma_0)}{\gamma_0} \equiv -\sum_{n=1}^{\infty} G'_n(\omega,\gamma_0)\sin n\boldsymbol{\tau} + G''_n(\omega,\gamma_0)\cos n\boldsymbol{\tau}. \tag{2.36}$$

The coefficients $\mathrm{G}'_\mathrm{n}(\omega,\gamma_0)$ and $(\mathrm{G}''_\mathrm{n}\omega,\gamma_0)$ are referred to as the *Fourier moduli* in equation [2.36], it should also be noted that $\gamma \equiv \omega t$.
In Equation [2.36] the Fourier moduli can be described in terms of odd powers of γ_0 which defines a matrix of frequency relying on non-linear moduli, this becomes :

$$\frac{\boldsymbol{\tau_{yx}}(\boldsymbol{\tau})}{\gamma_0} \equiv -\sum_{m=1}^{\infty}\sum_{n=1}^{m}\gamma_0^{m-1}[\mathrm{G'_{mn}}(\omega)\sin n\boldsymbol{\tau} + \mathrm{G''_{mn}}(\omega)\cos n\boldsymbol{\tau}]. \tag{2.37}$$

In equation [2.37] $\gamma \equiv \omega t$. When the response of LOAS to shear stress is expressed in odd powers of $\dot{\gamma}^0$, which expresses a matrix of frequency dependent on nonlinear viscosities it is expressed as :

$$\frac{\boldsymbol{\tau_{yx}}(\boldsymbol{\tau})}{\dot{\gamma}_0} \equiv -\sum_{n=1}^{\infty}\sum_{m=1}^{n}\dot{\gamma}^{0^{n-1}}[\boldsymbol{\eta'_{mn}}(\omega)\cos m\boldsymbol{\tau} + \boldsymbol{\eta''_{mn}}(\omega)\sin m\boldsymbol{\tau}]. \tag{2.38}$$

The variables $(\boldsymbol{\eta}^{'}_{mn})$, $(\boldsymbol{\eta}^{''}_{mn})$ are termed the storage and loss viscosities of the mnth order, with $(\boldsymbol{\eta}^{'}_{11})$, $(\boldsymbol{\eta}^{''}_{11}) \equiv (\boldsymbol{\eta}^{'})$, $(\boldsymbol{\eta}^{''})$. The harmonic stress is synonymous with the *'m'* in the mnth order while the n relates to the 1+ the power of expansion in the Equation [2.38].

[Saengow, Alan Jeffrey Giacomin, and Kolitawong 2015]

3. Generalized Newtonian models

The non-Newtonian viscosity as has been noticed is perhaps the most important property in macromolecular fluids; due to the fact of it's volatility by factors such as 10, 100 or even 1000. This means evidently that it's effect can't be ignored in practical situations in flow scenarios, lubrication and polymer processing applications. This lead to the development of the modification of the Newton's law of viscosity where the viscosity varies with the shear rate.

$$\tau_{yx} = -\mu\frac{\mathrm{d}v_x}{\mathrm{d}y}, \mu \text{ a constant for given temperature, pressure and composition} \tag{3.1}$$

$$\tau_{yx} = -\eta\frac{\mathrm{d}v_x}{\mathrm{d}y}, \eta \text{ is a function of } |\mathrm{d}v_x/\mathrm{d}y|. \tag{3.2}$$

With Equation [3.2] being the generalized Newtonian fluid formula which replaces the Newtonian fluid in Equation [3.1]. For the in-compressible Newtonian fluid $\tau = -\eta\dot{\gamma}$ where η is a function of the scalar invariants of $\dot{\gamma}$.

This equation gives accurate results for flow rates and shearing forces in steady shear flows it is applied to other complicated flows and systems with slow varying times.

[Robert Byron Bird, Armstrong, and Hassager 1987]

3–1. Power-law model

With respect to practical industrial applications the most essential region of the plot, log $\dot{\gamma}$ to the log η is the declining line curve also called the *'power-law region'* as shown in figure [3–1]. This can be described by the power-law formula:

$$\eta = m\dot{\gamma}^{n-1} \tag{3.3}$$

Consisting of two parameters m which has units of $\mathrm{Pa} \cdot \mathrm{s}^{\mathrm{n}}$ where n is dimensionless. With this model a wide range of analytical problems can be calculated making it most notable and widely-used in engineering work.

With a calculation of the power-law model it is easy to guess the effect of the non-Newtonian viscosity. But with all this is not a perfect model and has its short comings; [Robert Byron Bird, Armstrong, and Hassager 1987]

- For very small shear rates is not accurate and lead to errors.
- With just the two parameters of η and n is impossible to attain characteristic time and viscosity.
- Making a connection between the parameters m , η with the molecular weight and concentration is practically impossible.

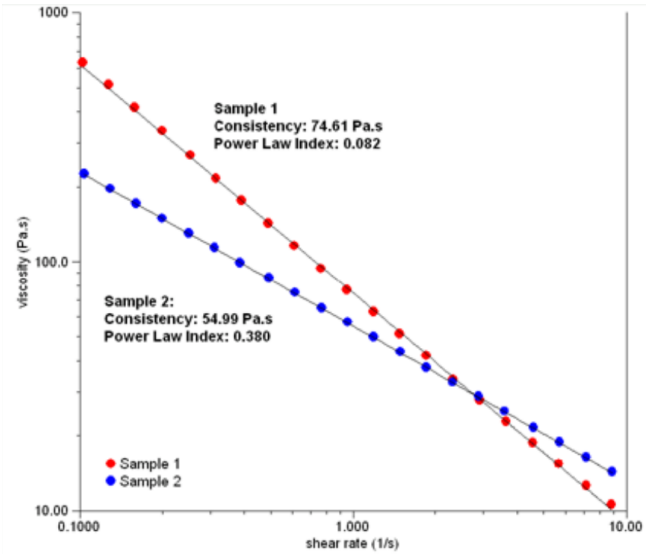

Figure 19: Power law model for two cosmetic curves

Power-law graph n.d.

3–2. Carreau-Yasuda Model

Determining analytical expressions for non-Newtonian viscosity curves, this model is almost indispensable and widely used for plotting numerical calculations. There are five unknown parameters in this model and is flexible enough to address different range of experimental curves.

$$\frac{\eta - \eta_\infty}{\eta_0 - \eta_\infty} = [1 + (\lambda\dot{\gamma})^a]^{(n-1)/a} \tag{3.4}$$

Considering the formula ; η_0 is the zero- shear rate, λ signifies a time constant, η_∞ is the infinite-shear-rate viscosity, n being the power-law exponent and a is the dimensionless parameter describing the region of changing from zero-shear to power law region.

There are just three parameters to be determined in this model namely; n, η_0 and λ. Regarding concentrated polymers the better results are attain when $a = 2$ and η_∞ is set to 0.

[Robert Byron Bird, Armstrong, and Hassager 1987]

4. Non-Newtonian physical fluids models

Based on mathematical derivatives only, it is impeccable to attain a deeper understanding on models in non-Newtonian fluid behaviour. This leads to the implementation of physical meaning to the mathematical models which are constructed to aid understanding. Based on physical theory, assumptions about molecular interactions at microscopical levels are scrutinized and magnified up. Focus is directed to dilute solutions, which mean that as the molecules of the polymer interact with one another they do have interaction with the solvent. With respect to dilute and concentrated solutions there are different properties at work which makes it vital to implore different models for the wide range of scenarios [Robert Byron Bird, Armstrong, and Hassager 1987].

Dumbbell models

The Dumbbell Models are applied for dilute polymeric solutions where there is more interaction between the polymers and the solvent. These models uses a two-bead spherical connection by a spring or rod to represent a polymer molecule [Robert Byron Bird, Armstrong, and Hassager 1987].

These models become practical since polymers have the tendency to contract, deform and expand as real molecules do and represented comprehensibly by them.

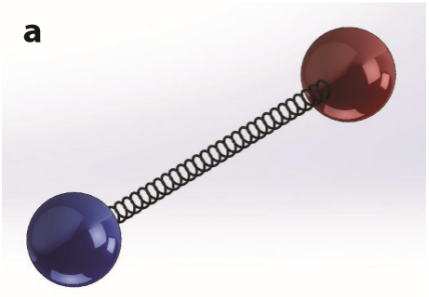

Figure 20: A simple elastic dumbbell model [R Byron Bird and A Jeffrey Giacomin 2016]

4–1. Hookean Dumbbells

A simple kinetic version of this model for a dilute solution of linear polymer consist of two beads which are connected by a Hookean spring. The force between them are considered linear with the strings adhering to the Hooke's law.

$$\boldsymbol{F} = H\boldsymbol{Q} \tag{4.1}$$

The force of the spring is represented by $\boldsymbol{F}$, H is the stiffness of the spring and $\boldsymbol{Q}$ being the vector between the beads. The beads bring into light the viscous forces and the spring, the elastic forces in the molecules. The downside of this model is it's simplicity, it does not factor in shear thinning, non-linearity and finite extensibility of molecules in real life applications [Robert Byron Bird, Armstrong, and Hassager 1987].

4–2. Finitely Elongated Nonlinear Elastic (FENE) Dumbbell

Among the many ways to model the behaviour of polymer solutions is the FENE dumbbell model. The finitely elongated Nonlinear Elastic Dumbbell model was proposed by Warner who wasn't content with the linear elastic spring model which has a limited expansion. He proposed a non-linear elastic model with the connector force linear at very small extensions but limited at high extensions.

$$\boldsymbol{F} = \frac{H\boldsymbol{Q}}{(1 - Q/Q_0)^2} \qquad Q < Q_0 \tag{4.2}$$

Where:

- $\boldsymbol{F}$ is the connector force.
- $\boldsymbol{Q}$ is the dimensional connector of the beads.
- Q_0 is the maximum strength of the spring
- H is the spring constant

When Q is at relatively small values it diminishes to the Hookean model, but if it increases it can't exceed Q_0. The model predicts quantitatively for non-Newtonian flow. The downside of this model is the absence of analytical solutions and a closed equation for stress sensor [Robert Byron Bird, Armstrong, and Hassager 1987].

4–3. FENE-P Dumbbell Model

In this model Perterlin whose name the model bears (P as in abbreviation FENE-P), proposed a replacement of the average elastic force by an average square value referred to as the Peterlin's closure.

The stress tensor for the model ;

$$\boldsymbol{\tau} = \boldsymbol{\tau}_s + \boldsymbol{\tau}_p. \tag{4.3}$$

The subscript s signifying the solvent distribution and p polymer contribution in Equation(4.3). To solve for the solvent distribution the following expression is used:

$$-\dot{\gamma} = Z\boldsymbol{\tau_p} + \frac{C_3}{2}\boldsymbol{\tau_p} - \left(\frac{C_3}{2}\boldsymbol{\tau}_p - \boldsymbol{\delta}\right)\frac{\mathrm{D}\ln Z}{\mathrm{D}t} \tag{4.4}$$

$$Z = C_1\frac{2C_2}{C_3}tr(\boldsymbol{\tau}_p) \tag{4.5}$$

With C_1, C_2, C_3 being constant and parameters that varies with the polymer of choice.

4–4. FENE-P Bead-Spring-Chain

This model represents an extension from the original FENE-P dumbbells model. The assumption is that the polymer molecules are represented by chain of beads and connected by elastic FENE springs.

4–5. C-FENE-P Dumbbell Model

The FENE dumbbell model can be applied if the solution has been diluted enough to enhance a close interaction between the polymer molecules and the molecules of the solvent. Isotropic stokes law with the independent coefficient ζ describes the degree of interaction between the former and later. Three main parameters contribute to the stress tensor of the solution namely; ideal gas pressure nkT, dimensionless non-linearity parameter b and a time constant λ [Shogin and Amundsen 2019].

$$\begin{aligned} P &= nkT \\ b &= HQ_0^2/kT \\ \lambda &= \lambda_Q = \frac{\zeta Q_0^2}{12kT} \end{aligned} \tag{4.6}$$

Where n is the concentration number of the dumbbells , k Boltzmann's constant and T thermodynamic temperature. Electric impulse between the charged parts of the poly-electrolyte chain is qualitatively characterized with the assumption of effective charges q and relative permittivity ε, modifying the force connecting with an electrostatic Coulomb force [Shogin and Amundsen 2019].

$$\boldsymbol{F}_c = \frac{H\boldsymbol{Q}}{1-(Q/Q_0)^2} - \frac{q^2}{4\pi\varepsilon_0\varepsilon}\frac{\boldsymbol{Q}}{Q^3}. \tag{4.7}$$

The difference between the C-FENE-P dumbbell and the FENE-P dumbbel is the introduction of E which is attributed to the C-FENE-P characterizing the rigidity of poly-electrolyte molecules; the greater E is the more rigid the molecules are anticipated to be. It also account for salt sensitivity where it is inversely related. The "C" in the abbreviation C-FENE-P model stands for *charged* [Shogin and Amundsen 2019] *to be published in physics of fluids* (2020).

$$E = \frac{q^2/4\pi\varepsilon_0\varepsilon Q_0}{kT}. \tag{4.8}$$

4–6. Phan-Thien-tanner models (PTT)

This model is formulated based on a constitutive equation from a Lodge-Yamamoto type of network theory for polymeric fluids. The theory explains how thermal forces at equilibrium causes the junctions of the network to be broken and reformed as depicted in figure [21]. The rate at which the network deforms is slow as compared to the rate of motion and the time of junction breakage and reformation, hence the model is at equilibrium at all times [Gupta and Kothari 2012].
The rate at which breakage and reformation of the joints occurs is related to the average extension of the network's strand. Every network strand is represented by the vector $\boldsymbol{\rho}$.

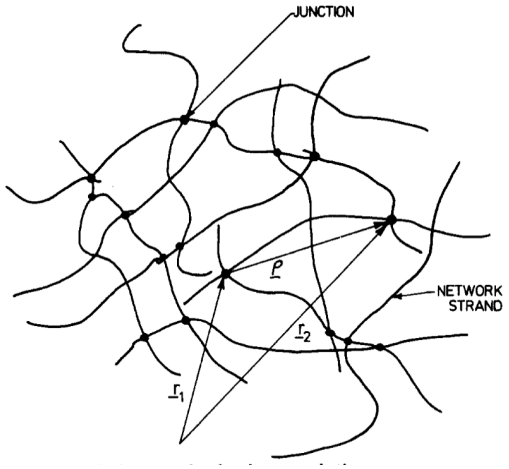

Figure 21: Typical network of polymer solutions

It gives a description of the behaviour of concentrated solutions; thus when polymer molecules are strongly incline to each other than the solvent. The model is able to predict stress overshoot accurately even at high shear rates. During elongational flow the Trouton viscosity is finite for all elongational rates [Thien and Tanner 1977].
Mathematically, a simplified version of a non-affine PTT model has the form :

$$\dot{\boldsymbol{\rho}} = \mathrm{L}\rho - \sigma\rho - \xi\mathrm{D}\rho, \tag{4.9}$$

where the variables ξ and σ are constants and L is the velocity gradient tensor.

The model is appealing with respect to the fact that, there are two dimensionless parameters which can be determined from the experiment i.e. ξ obtained from the viscometric flows and ϵ derived from the elongational experiments making control of both flow reactions possible [Thien and Tanner 1977].

The general equation for a PTT single model can be expressed as :

$$Z(tr\boldsymbol{\tau}) \cdot \boldsymbol{\tau} + \lambda \boldsymbol{\tau_{(1)}} + \frac{\xi}{2}\{\gamma \cdot \boldsymbol{\tau} + \boldsymbol{\tau} \cdot \dot{\gamma}\} = -\eta_0 \dot{\gamma}. \tag{4.10}$$

PPT models are classified as either simplified (affine) ($\xi = 0$) or non-affine ($\xi \neq 0$). Also they can be termed as linear or exponential with respect to the Z.

- The model is termed linear if:

$$Z = 1 - \frac{\epsilon\lambda}{\eta_0}\mathrm{tr}\boldsymbol{\tau} \tag{4.11}$$

- And in exponential Z takes the form :

$$Z = \exp\left[\frac{\epsilon\lambda}{\eta_0}\mathrm{tr}\boldsymbol{\tau}\right] \tag{4.12}$$

ϵ signifies the extensional parameter, λ the relaxation time and η_0 the zero-shear rate viscosity.

A distinguishing feature of this model is that of product-logarithmic shear thinning it exhibits; where there is a simultaneous increase in the shear rate and the thinning but no power-law region exist.

Figure [22] give a visual representation of the linear and exponential behaviour of Phan-Thien-Tanner:

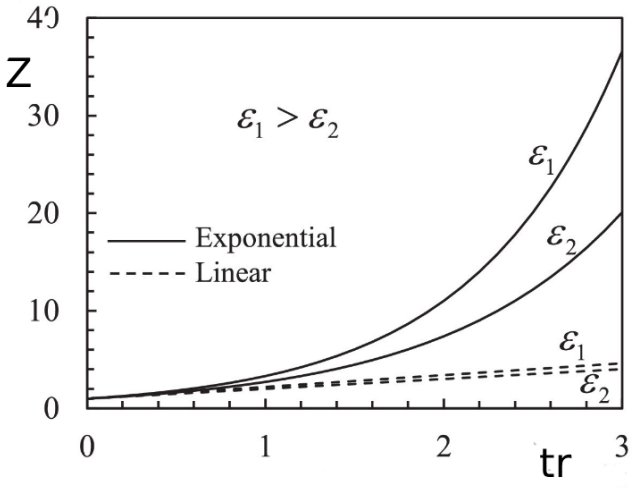

Figure 22: Dependancy of Z to tr in exponential and linear PTT models [Ferrás et al. 2019]

5. Rheological behaviour analysis of polymers

5–1. Linear and exponential Phan-Thien-Tanner models

For the purpose of this research we concentrate and explore the simple *(affine)* where ($\xi = 0$) linear and exponential Phan-Thien-Tanner (PTT) models. A single mode of the PTT models for both linear and exponential are expressed as follows:

$$\left(1 - \frac{\epsilon\lambda}{\eta_0} tr\boldsymbol{\tau}\right)\boldsymbol{\tau} + \lambda\boldsymbol{\tau_{(1)}} = -\eta_0\dot{\gamma} \tag{5.1}$$

$$\exp\left(\frac{\epsilon\lambda}{\eta_0} tr\boldsymbol{\tau}\right)\boldsymbol{\tau} + \lambda\boldsymbol{\tau_{(1)}} = -\eta_0\dot{\gamma} \tag{5.2}$$

Where tr is the trace of the stress tensor, η_0 is the polymeric viscosity and λ is the relaxation time. As noticed Equation[5.1] is quadratic with regard to stress tensor components and Equation [5.2] is in exponential form. This is very essential as it is the underlying feature distinguishing the PTT model from the other models. Also from the original model proposed by Phan-Thein and Tanner, a small positive rational number is ascribed to ε and it can be in the order of 10^{-2}, which is valid from $0 < \varepsilon < 0.25$. For better visual quality of the plots $\varepsilon = 0.1$.
[Shogin 2020]

- $\boldsymbol{\tau}$: anisotropic stress tensor
- $\dot{\boldsymbol{\gamma}}$: the rate of stain tensor
- $\boldsymbol{\tau_{(1)}}$: upper-convected time derivative
- η_0 : zero-shear-rate viscosity
- ϵ : extensibility parameter
- tr : trace of the stress tensor

In table 1 the forms of the stress tensor, rate of strain, velocity field and corresponding Oldroyd derivative for simple shear flow is presented. To attain the formula for steady start-up shear flow, the parameters in Table 1 are substituted into Equations [5.1] and [5.2] :

Table 1: Forms of velocity field $\boldsymbol{\varepsilon}$, rate of strain stress tensor $\dot{\boldsymbol{\gamma}}$, stress tensor $\boldsymbol{\tau}$ and oldroyd derivative $\boldsymbol{\tau_{(1)}}$ for Shear flow.

$\boldsymbol{v}$	$\dot{\boldsymbol{\gamma}}$	$\boldsymbol{\tau}$	$\boldsymbol{\tau_{(1)}}$
$[\dot{\gamma}\ x_2,\ 0,\ 0]$	$\begin{bmatrix} 0 & \dot{\gamma} & 0 \\ \dot{\gamma} & 0 & 0 \\ 0 & 0 & 0 \end{bmatrix}$	$\begin{bmatrix} \tau_{11} & \tau_{12} & 0 \\ \tau_{12} & \tau_{22} & 0 \\ 0 & 0 & \tau_{33} \end{bmatrix}$	$\partial_t \boldsymbol{\tau}$ - $\begin{bmatrix} 2\tau_{12} & \tau_{22} & 0 \\ \tau_{22} & 0 & 0 \\ 0 & 0 & 0 \end{bmatrix} \dot{\gamma}$

Substituting values from Table 1 into Equations [5.1] and [5.2] respectively gives :

$$\left(1 - \frac{\epsilon\lambda}{\eta_0} tr\boldsymbol{\tau}\right) \begin{bmatrix} \tau_{11} \\ \tau_{12} \\ \tau_{22} \\ \tau_{33} \end{bmatrix} + \lambda \frac{\mathrm{d}}{\mathrm{d}t} \begin{bmatrix} \tau_{11} \\ \tau_{12} \\ \tau_{22} \\ \tau_{33} \end{bmatrix} = \begin{bmatrix} 2\lambda\tau_{12}\dot{\gamma}_0 \\ -\eta_0\dot{\gamma}_0 \\ 0 \\ 0 \end{bmatrix} \tag{5.3}$$

$$\exp\left(\frac{\epsilon\lambda}{\eta_0} tr\boldsymbol{\tau}\right) \begin{bmatrix} \tau_{11} \\ \tau_{12} \\ \tau_{22} \\ \tau_{33} \end{bmatrix} + \lambda \frac{\mathrm{d}}{\mathrm{d}t} \begin{bmatrix} \tau_{11} \\ \tau_{12} \\ \tau_{22} \\ \tau_{33} \end{bmatrix} = \begin{bmatrix} 2\tau_{12}\dot{\gamma}_0 \\ -\eta_0\dot{\gamma}_0 \\ 0 \\ 0 \end{bmatrix} \tag{5.4}$$

The material functions which describes the diverse behaviour of the fluid at steady, initiation and cessation regimens of the shear flows are presented in Table [2]. Regarding step-rate related material functions, new terms are assigned. A collective name for initiation flows are hereby referred to as "stress growth functions" while for cessation flows - "stress relaxation functions"[Shogin 2020].

Table 2: Definitions of the material functions related to the steady, initiation and cessation regimes of shear flow

Steady flow regime	Start-up(+)and cessation(-) regimes
$\boldsymbol{\eta}(\dot{\boldsymbol{\gamma}}) = -\dfrac{\boldsymbol{\tau}_{12}(\dot{\boldsymbol{\gamma}})}{\dot{\boldsymbol{\gamma}}}$	$\boldsymbol{\eta}^{\pm}(t, \dot{\gamma}_0) = -\dfrac{\boldsymbol{\tau}_{12}(t, \dot{\boldsymbol{\gamma}}_0)}{\dot{\boldsymbol{\gamma}}_0}$
$\boldsymbol{\Psi_1}(\dot{\boldsymbol{\gamma}}) = -\dfrac{\boldsymbol{\tau}_{11}(\dot{\boldsymbol{\gamma}}) - \boldsymbol{\tau}_{22}(\dot{\boldsymbol{\gamma}})}{\dot{\boldsymbol{\gamma}}^2}$	$\boldsymbol{\Psi}_{\mathbf{1}}^{\pm}(t, \dot{\boldsymbol{\gamma}}_0) = -\dfrac{\boldsymbol{\tau}_{11}(t, \dot{\boldsymbol{\gamma}}) - \boldsymbol{\tau}_{22}(t, \dot{\boldsymbol{\gamma}})}{\dot{\boldsymbol{\gamma}}_0^2}$
$\boldsymbol{\Psi_2}(\dot{\boldsymbol{\gamma}}) = -\dfrac{\boldsymbol{\tau}_{22}(\dot{\gamma}) - \tau_{33}(\dot{\gamma})}{\dot{\boldsymbol{\gamma}}^2}$	$\boldsymbol{\Psi}_{\mathbf{2}}^{\pm}(t, \dot{\boldsymbol{\gamma}}_0) = -\dfrac{\boldsymbol{\tau}_{22}(t, \dot{\boldsymbol{\gamma}}_0) - \boldsymbol{\tau}_{33}(t, \dot{\boldsymbol{\gamma}}_0)}{\dot{\boldsymbol{\gamma}}_0^2}$

5–1.1. Dimensionless formulation

To enhance a comprehensive and visual analysis of the Equations [5.3] and [5.4], all time variables will be substituted with a dimensionless one r [Shogin 2020].
Where r will be defined as :

$$r = t/\lambda \tag{5.5}$$

As a result of this any physical quantity X becomes,

$$\frac{\mathrm{d}X}{\mathrm{d}t} = \frac{1}{\lambda}\frac{\mathrm{d}X}{\mathrm{d}r} \equiv \frac{1}{\lambda}X' \tag{5.6}$$

Furthermore, the Weissenberg number(Wi) together with the dimensionless combinations of stress tensor components ($\mathbb{N}$, $\mathbb{S}$) are introduced for the initiation flow. Dimensionless flow combinations depend on the flow type and since we are considering start up of steady shear flow the definitions of the expressions are: [Shogin 2020]

$$\mathrm{Wi} = \lambda\dot{\gamma}_0 \tag{5.7}$$

$$\begin{bmatrix} \mathbb{N}_1 \\ \mathbb{S} \end{bmatrix} = -\frac{\varepsilon}{\eta_0\dot{\gamma}} \begin{bmatrix} \tau_{11} \\ \tau_{12} \end{bmatrix}. \tag{5.8}$$

For a simple shear flow the start-up and steady-flow material functions can be related to the dimensionless combinations of stress tensor components by the expressions:

$$\begin{bmatrix} \eta^+(r,\mathrm{Wi}) \\ \boldsymbol{\Psi}_1^+(r,\mathrm{Wi}) \\ \eta(\mathrm{Wi}) \\ \boldsymbol{\Psi}_1(\mathrm{Wi}) \end{bmatrix} = \frac{\eta_0}{\varepsilon} \begin{bmatrix} \mathbb{S} \\ \lambda\mathbb{N}_1/\mathrm{Wi} \\ \sigma \\ \lambda\delta_1/\mathrm{Wi} \end{bmatrix}. \tag{5.9}$$

These dimensionless formulation apply to both the linear and exponential Phan-Thien-Tanner (PTT) models and will be very instrumental in the graphical representation.

5–1.2. Steady shear flow solutions

Before solving for the differential Equations [5.5] and [5.6] their algebric flow variants are considered. The time dependant material functions for start-up flows are easily expressed in dimensionless stress tensor components which relate to their corresponding steady flow [Shogin 2020]
Equations 5.3 and 5.4 becomes combined with the dimensionless equations of 5.7 and 5.9 transforms to :

$$-(1+\mathrm{Wi}\mathbb{N}_1)\mathbb{N}_1+2\mathrm{Wi}\mathbb{S} \implies (1+\mathrm{Wi}\delta_1)\delta_1=2\mathrm{Wi}\sigma, \tag{5.10}$$

$$-(1+\mathrm{Wi}\mathbb{N}_1)\mathbb{S}+\varepsilon \implies (1+\mathrm{Wi}\delta_1)\sigma=\varepsilon. \tag{5.11}$$

$$\delta_1=\frac{2}{\varepsilon}\mathrm{Wi}\sigma^2 \tag{5.12}$$

The linear and exponential models of PPT finally yields

$$\sigma=\frac{1}{\mathrm{Wi}}\sqrt{\frac{2\varepsilon}{3}}\sinh\left[\frac{1}{3}\operatorname{arcsinh}\left(3\sqrt{\frac{3\varepsilon}{2}}\mathrm{Wi}\right)\right] \tag{5.13}$$

$$\sigma_{exp}=\frac{\sqrt{\varepsilon}\sqrt{\mathrm{Productlog}\left[4\mathrm{Wi}^2\varepsilon\right]}}{2\mathrm{Wi}} \tag{5.14}$$

With the aid of Equations 5.14 and 5.13 , $\delta_1(\mathrm{Wi})$ can be calculated with Equation 5.12.

The asymptotic behaviour of the shear viscosity curve can be analysed using Equations 5.13 and 5.14 as $\mathrm{Wi}\to 0, \sigma\to\varepsilon$; this means that $\eta\to\eta_0$ while $\mathrm{Wi}\to 0$. Approximately, $\sigma\sim\sqrt[3]{\varepsilon^2/2}\mathrm{Wi}^{-\frac{2}{3}}$ and therefore $\eta\sim\eta_0\sqrt[3]{1/2\varepsilon}\mathrm{Wi}^{-\frac{2}{3}}$.

[Shogin 2020]

Advance modelling with Wolfram Mathematica

In order to have an in-depth overview and visual representation of the models Wolfram Mathematica (also called *Mathematica*) is employed. Mathematica is a symbolic mathematical computation program, sporadically referred to as a computer algebra program which has a wide range of use spanning over scientific, mathematical, engineering and computing disciplines. In technical spheres like machine learning, image processing, data science, visualizations, etc it is very nifty. Stephen Wolfram conceived the concept initially in the year 1988 and the program has since being developed by Wolfram Research of Champaign, Illinois. Mathematica uses the Wolfram language to execute commands [*Wolfram Mathematica* n.d.].

With Mathematica, the steady shear flow solutions which has been derived in Equations 5.13 and 5.14 can be coded and graphs generated for further analysis.

Example of Mathematica code : Figure [23] shows how a typical code in Mathematica for a linear Phan-their-tanner model looks like, the result produced is in Figures [24,25].

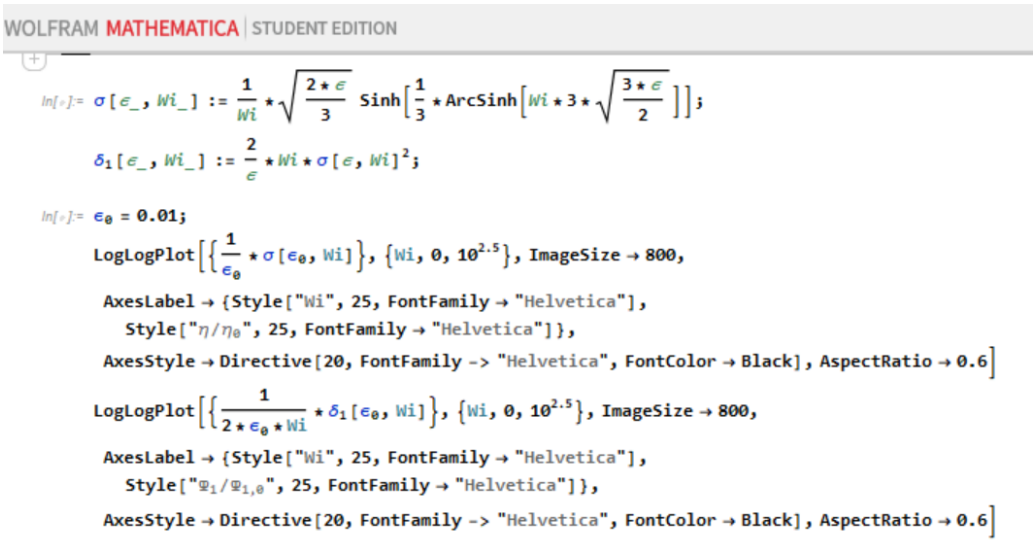

Figure 23: Typical Mathematica code for a linear PPT model

.

Shear stress growth function of linear PPT model : In figure [24] it is noticed that the shear stress decreases gradually with increasing Wi numbers, initially at a very gentle rate but from Wi ≥ 5 it takes a very steep slope.

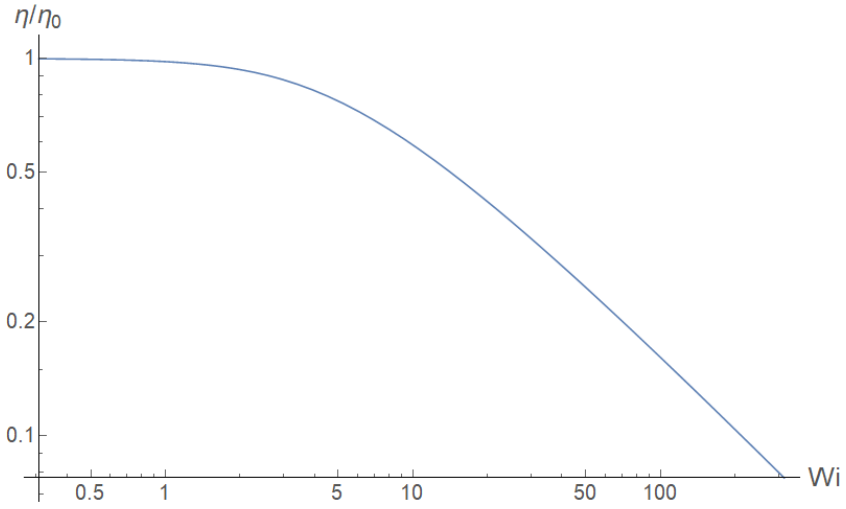

Figure 24: Shear stress growth function η/η_0 for linear PTT model as a function of Wi

.

First normal stress growth function of linear PPT model : The First normal stress growth function in figure [25] also exhibits a similar behaviour not very much different from the shear stress function. It reluctantly decreases with increasing Wi numbers and take a steep toll when Wi ≥ 5.

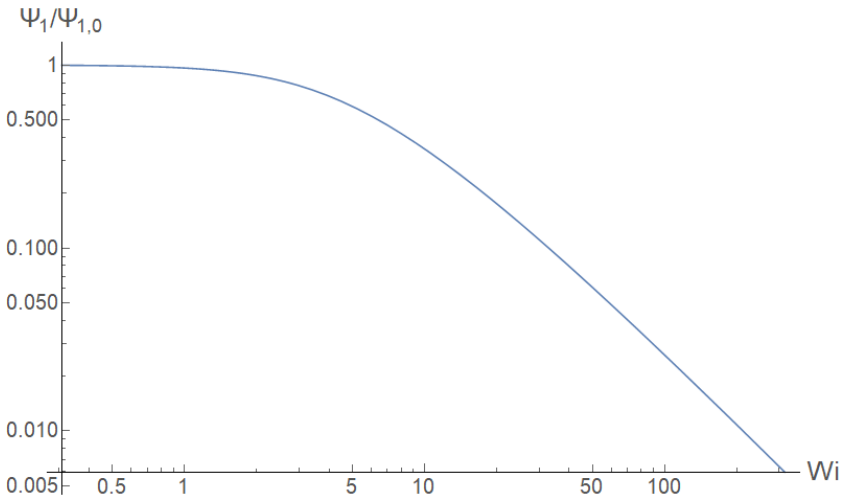

Figure 25: First normal stress difference growth function $\mathbf{\Psi}_1/\mathbf{\Psi}_{1.0}$ of Linear PPT model as a function of Wi

.

Shear stress function of exponential PTT model : The behaviour of the exponential shear stress function as shown in the figure [26] shows an extended, close-to-linear curves initially. But as the linear model it takes a sharp decent around Wi ≥ 5.

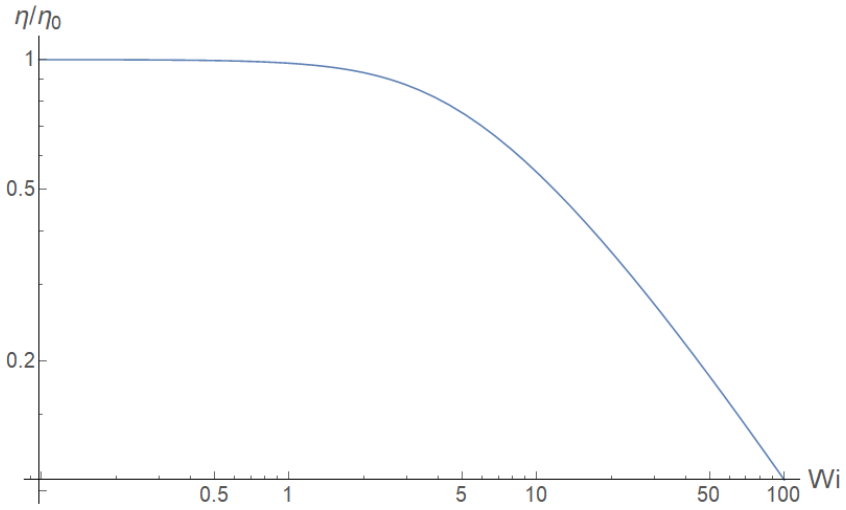

Figure 26: Shear stress growth function η/η_0 for exponential PTT model as a function of Wi

First normal stress growth function : This also follows suit with the linear models and decent abruptly with the increase in Wi numbers as shown in figure [27], but the curve is much smoother than the shear stress exponential model.

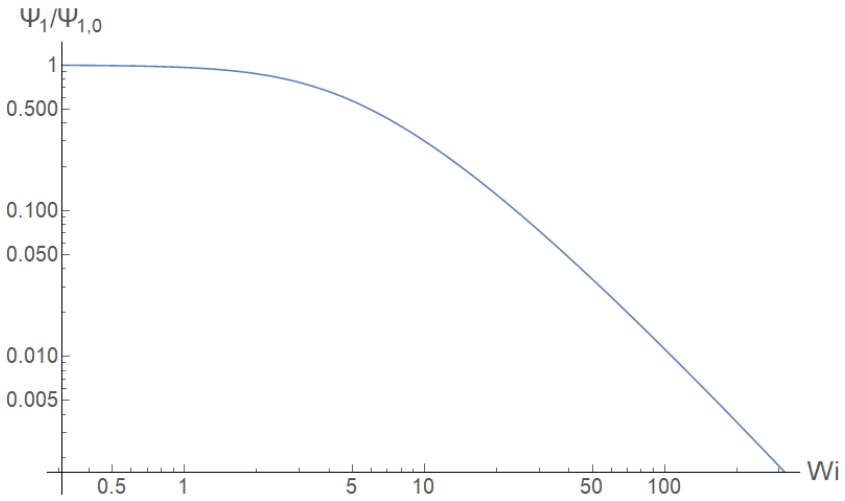

Figure 27: First normal stress difference growth function $\mathbf{\Psi}_1/\mathbf{\Psi}_{1.0}$ of exponential PPT model as a function of Wi

Normalized stress growth functions : The graphs in figure [28] and [29] shows the behaviour of the normalized transient viscosity and first normal stress coefficient functions at different Wi numbers 1.5, 15 and 150. The influence the Wi number exerts on the material function is evident.
Except for the limiting scenarios where $Wi \to 0$ the curves exhibit an oscillatory behaviour not easily seen apart from the first overshoot at start-up. At high Wi numbers both of the functions experience a a quasi-periodic, exponentially damped oscillation while approaching one. [Shogin 2020]

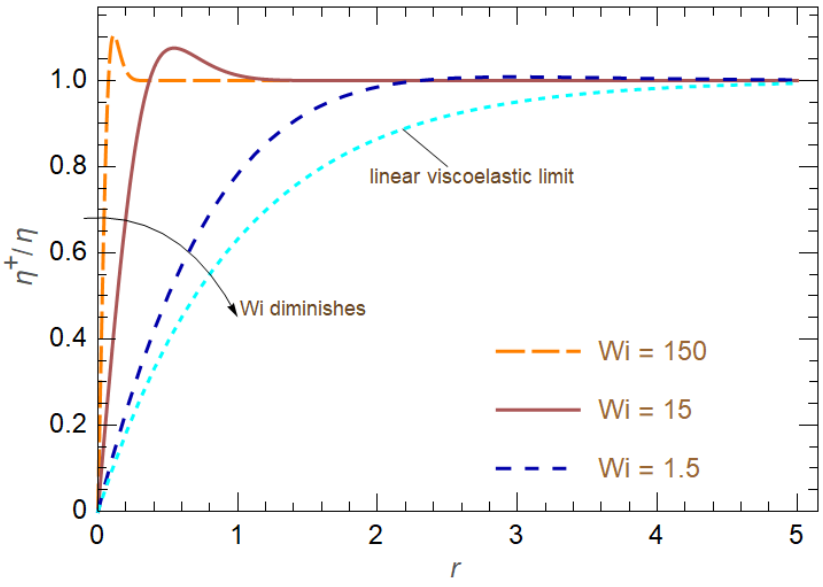

Figure 28: Transient Viscosity at start-up of steady shear flow, normalized with respect to their steady flow values. Exact expression obtained from the linear PPT model as function of dimensionless time for different Weissenberg numbers

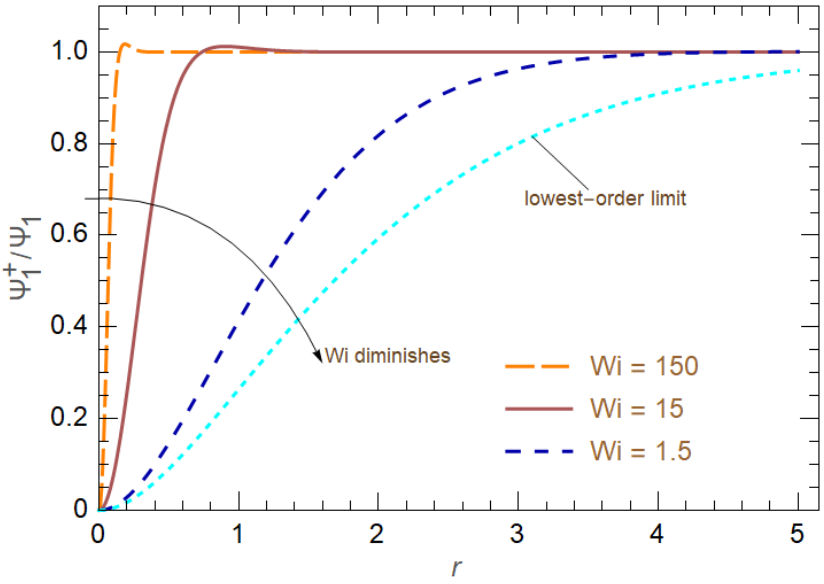

Figure 29: First normal stress coefficient at start-up of steady shear flow, normalized with respect to their steady flow values. Exact expression obtained from the linear PPT model as function of dimensionless time for different Weissenberg numbers

Cessation of steady shear : In figure [30] the behaviour of the normalised stress relaxation functions is shown. It diminishes and approaches 0 uniformly at different Wi numbers. At higher Wi there is a faster, exponential decease toward 0, whiles at lower Wi the decease in the function as it approaches 0 is lesser.

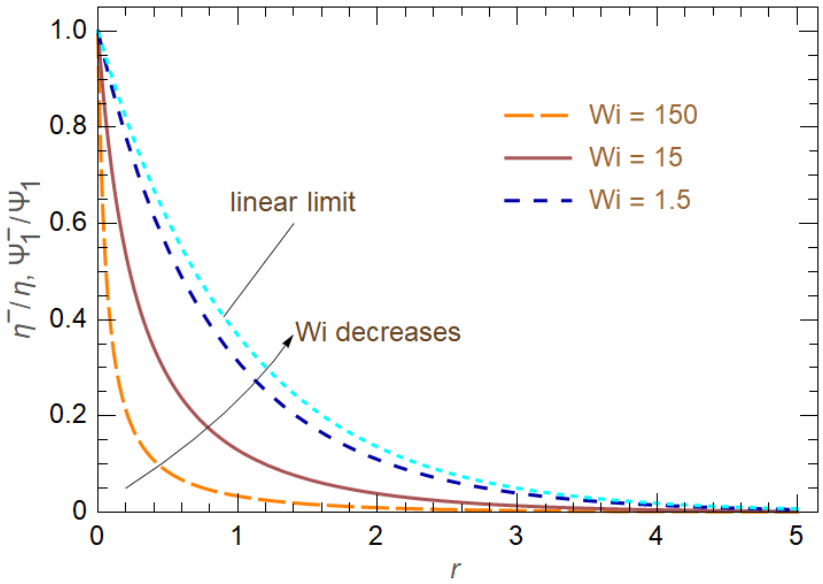

Figure 30: The stress relaxation functions at cessation of steady shear flow, normalized with respect to their steady flow values. Exact expression for the linear PTT model as a function of dimensionless time at different Weissenberg numbers.

In figures [31] and [32] the behavior of the normalized stress growth functions as a function of the dimensionless time while the Wi numbers are adjustable is shown. When the $Wi = 0.01$ both functions approaches to 1 but as Wi increases the functions bend simultaneously to 0.

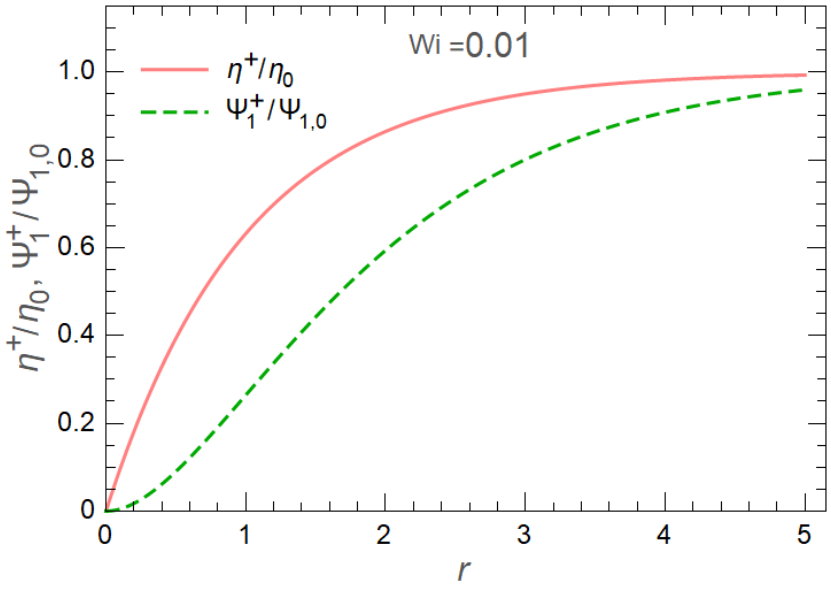

Figure 31: The stress relaxation functions at cessation of steady shear flow of the linear PTT model as a function of dimensionless time at Wi = 0.01

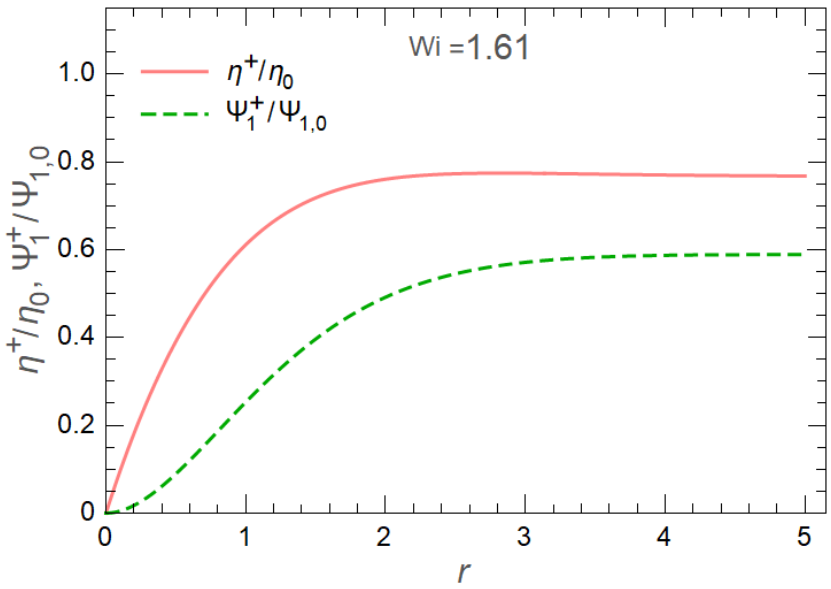

Figure 32: The stress relaxation functions at cessation of steady shear flow of the linear PTT model as a function of dimensionless time at Wi = 1.61

5–2. Linear and exponential modules for large amplitude oscillation shear flow (LAOS)

To begin with, the linear and exponential modules for steady shear flow in LAOS are considered, they are expressed as

$$\left(1-\frac{\varepsilon\lambda}{\eta_0}\mathrm{tr}\boldsymbol{\tau}\right)\boldsymbol{\tau}+\lambda\boldsymbol{\tau_1}=2\lambda\boldsymbol{\tau}\dot{\boldsymbol{\gamma}} \tag{5.15}$$

$$\left(1-\frac{\varepsilon\lambda}{\eta_0}\mathrm{tr}\boldsymbol{\tau}\right)\boldsymbol{\tau}+\lambda\boldsymbol{\tau_1}=-\eta_0\dot{\boldsymbol{\gamma}} \tag{5.16}$$

Where tr is the trace of the stress tensor, η_0 is the polymeric viscosity and λ is the relaxation time. As noticed the equations [5.19] and[5.20] are almost identical to each other differing only on the right hand of the equations.

- $\boldsymbol{\tau}$: anisotropic stress tensor
- $\dot{\boldsymbol{\gamma}}$: the rate of stain tensor
- $\boldsymbol{\tau}_{(1)}$: upper-convected time derivative
- η_0 : zero-shear-rate viscosity
- ϵ : extensibility parameter
- tr : trace of the stress tensor

Referring from table [1] section [5–1], parameters are substituted into equations [5.20] and [5.19]

$$\left(1-\frac{\epsilon\lambda}{\eta_0}tr\boldsymbol{\tau}\right)\begin{bmatrix}\tau_{11}\\ \tau_{12}\\ \tau_{22}\\ \tau_{33}\end{bmatrix}+\lambda\frac{\mathrm{d}}{\mathrm{d}t}\begin{bmatrix}\tau_{11}\\ \tau_{12}\\ \tau_{22}\\ \tau_{33}\end{bmatrix}=\begin{bmatrix}2\lambda\tau_{12}\dot{\gamma}_0\\ 0\\ 0\\ 0\end{bmatrix} \tag{5.17}$$

$$\left(1-\frac{\epsilon\lambda}{\eta_0}tr\boldsymbol{\tau}\right)\begin{bmatrix}\tau_{11}\\ \tau_{12}\\ \tau_{22}\\ \tau_{33}\end{bmatrix}+\lambda\frac{\mathrm{d}}{\mathrm{d}t}\begin{bmatrix}\tau_{11}\\ \tau_{12}\\ \tau_{22}\\ \tau_{33}\end{bmatrix}=\begin{bmatrix}-\eta_0\dot{\gamma}_0\\ 0\\ 0\\ 0\end{bmatrix} \tag{5.18}$$

$\tau_{22}=\tau_{33}=0$ and are identical, hence the trace of the stress tensor $(\mathrm{tr}\boldsymbol{\tau})=\tau_{11}+\tau_{22}+\tau_{33}=\tau_{11}$.

Hence the equations reduces to

$$\lambda\frac{\mathrm{d}}{\mathrm{dt}}\boldsymbol{\tau}_{11}+\left(1-\frac{\varepsilon\lambda}{\eta_0}\mathrm{tr}\tau\right)\boldsymbol{\tau}_{11}=2\lambda\boldsymbol{\tau}_{11}\dot{\boldsymbol{\gamma}} \tag{5.19}$$

$$\lambda\frac{\mathrm{d}}{\mathrm{dt}}\boldsymbol{\tau}_{11}+\left(1-\frac{\varepsilon\lambda}{\eta_0}\mathrm{tr}\tau\right)\boldsymbol{\tau}_{12}=-\eta_0\dot{\boldsymbol{\gamma}} \tag{5.20}$$

In LAOS, oscillating shear flow is created when the the fluid is confined to a shear apparatus where one solid-liquid boundary is forced to undergo coplanar sinusoidal displacement. There are two constants which control the flow namely; the amplitude ($\dot{\gamma}_0$) and the frequency (ω), which yield an oscillating effect [Poungthong et al. 2019]

$$\dot{\gamma}=\dot{\gamma}_0\cos\omega\mathrm{t} \tag{5.21}$$

5–2.1. Dimensionless formulation

For the sake of convenience equations [5.17] and [5.18] are presented in dimensionless form. The time variables are replaced with a dimensionless one r to begin with

$$\frac{\mathrm{d}}{\mathrm{dt}}=\frac{\mathrm{d}}{\mathrm{dr}}*\frac{\mathrm{dr}}{\mathrm{dt}}=\omega\frac{\mathrm{d}}{\mathrm{dr}} \tag{5.22}$$

Furthermore, the Weissenberg number(Wi), Deborah number(De), with the dimensionless combinations of stress tensor components ($\mathbb{N}$, $\mathbb{S}$) are introduced for the initiation flow in equation [5.21]. Dimensionless flow combinations depend on the flow type and since we are considering start-up of steady shear flow, the definitions of the cosinusodal shear rate using characteristic relaxation time (λ) becomes

$$\lambda\dot{\gamma}_{yx}=\lambda\dot{\gamma}^0\cos\lambda\omega\left(\frac{t}{\lambda}\right)\equiv\mathrm{Wi}\cos\mathrm{De}\left(\frac{t}{\lambda}\right) \tag{5.23}$$

The dimensionless variables Wi and De are defined as follows

$$\mathrm{Wi}=\lambda\dot{\gamma}_0 \tag{5.24}$$

$$\mathrm{De}=\lambda\omega \tag{5.25}$$

Where λ is the characteristic relaxation time of the viscoelastic fluid, ω is the frequency and $\dot{\gamma}_0$ is the stain amplitude.

The dimensionless combinations of stress components $\mathbb{N}$ and $\mathbb{S}$ are expressed as follows:

$$\left[\mathbb{N}_1\right] = -\frac{1}{\eta_0\dot{\gamma}_0}\left[\tau_{11}\right] \tag{5.26}$$

$$\left[\mathbb{S}\right] = -\frac{1}{\eta_0\dot{\gamma}_0}\left[\tau_{12}\right] \tag{5.27}$$

5–2.2. Steady shear flow solutions

Substituting dimensionless time from equation [5.22] into equations [5.19] and [5.20] the following expression is deduced:

$$\lambda\omega\frac{\mathrm{d}}{\mathrm{dr}}\boldsymbol{\tau}_{11} + \left(1 - \frac{\varepsilon\lambda}{\eta_0}\mathrm{tr}\tau\right)\boldsymbol{\tau}_{11} = 2\lambda\boldsymbol{\tau}_{12}\dot{\boldsymbol{\gamma}}_0\cos r \tag{5.28}$$

$$\lambda\omega\frac{\mathrm{d}}{\mathrm{dr}}\boldsymbol{\tau}_{11} + \left(1 - \frac{\varepsilon\lambda}{\eta_0}\mathrm{tr}\tau\right)\boldsymbol{\tau}_{12} = -\eta_0\dot{\boldsymbol{\gamma}}_0\cos r \tag{5.29}$$

Also, the dimensionless combinations are incorporated from equations [5.26] and [5.27] together with the Wi and De numbers

$$\mathrm{De}\frac{\mathrm{d}}{\mathrm{dr}}\mathbb{N}_1 + (1 + \varepsilon\mathrm{Wi}\mathbb{N}_1)\mathbb{N}_1 = 2\mathrm{Wi}\mathbb{S}\cos r \tag{5.30}$$

$$\mathrm{De}\frac{\mathrm{d}}{\mathrm{dr}}\mathbb{S} + (1 + \varepsilon\mathrm{Wi}\mathbb{N}_1)\mathbb{S} = 1 \tag{5.31}$$

5–2.3. Ewoldt grids

For a comprehensive analysis and confirmation of the accuracy of equations [5.30] and [5.31] the Ewoldt grid is incorporated in plotting the graphs for normal stress difference to the $\mathrm{Wi}\cos(\omega\mathrm{t})$ for both the linear and exponential LAOS models.

Each loop is made under specific conditions for Wi and De and graphed into rows and columns which are termed as Pipkin space. This is done as Wi is plotted against De in the graph and it is termed as the *Ewoldt grid.*[Poungthong et al. 2019]

Advance modelling for linear large amplitude oscillation shear (LAOS) model using Mathematica

Using Mathematica and equation [5.30] the figures are produced for the linear LAOS module. The figures are grouped into constant De numbers and varying Wi numbers. The values of De numbers are 0.1,1 and 5.

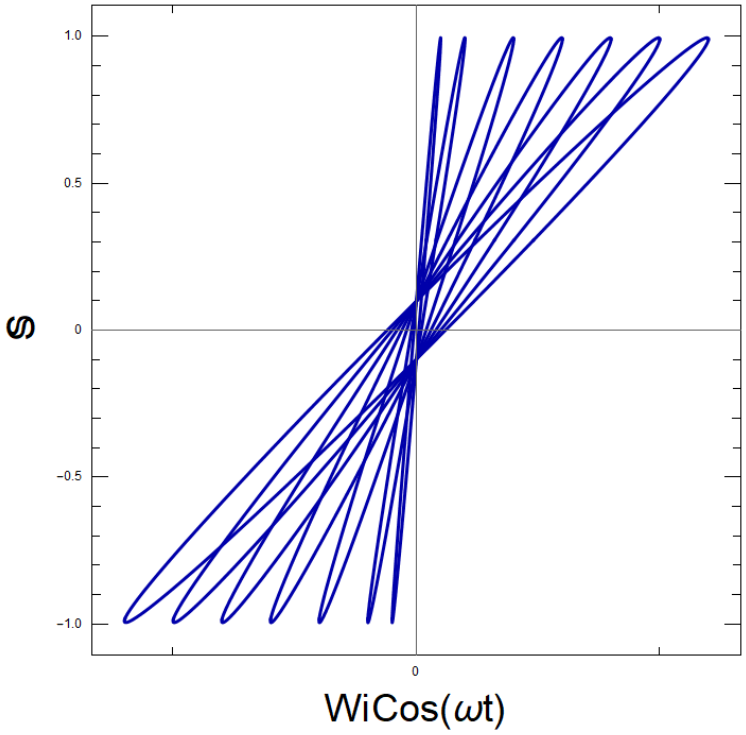

Figure 33: Dimensionless shear stress verses dimensionless shear rate. Where $\frac{\text{Wi}}{\text{De}} = (0.1, 0.2, 0.4, 0.6, 0.8, 1, 1.2)$ and $\text{De} = 0.1$

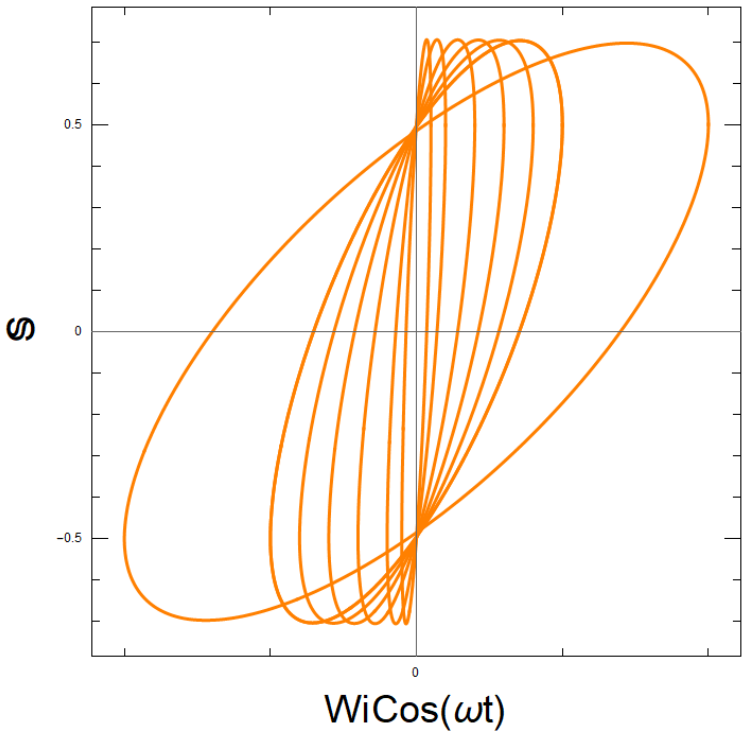

Figure 34: Dimensionless shear stress verses dimensionless shear rate. Where $\frac{\text{Wi}}{\text{De}} = (0.1, 0.2, 0.4, 0.6, 0.8, 1, 1.2)$ and $\text{De} = 1$

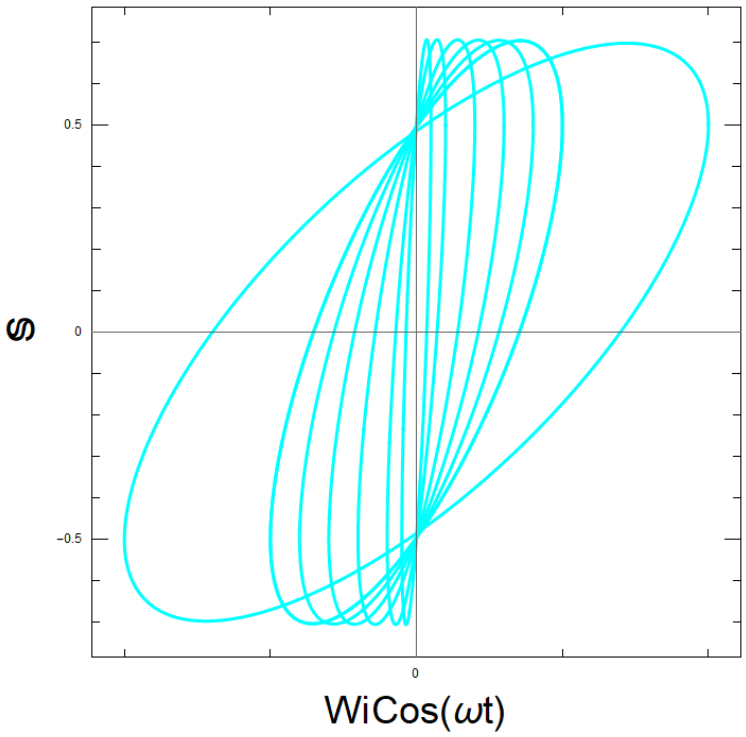

Figure 35: Dimensionless shear stress verses dimensionless shear rate. Where $\frac{\text{Wi}}{\text{De}} = (0.1, 0.2, 0.4, 0.6, 0.8, 1, 1.2)$ and $\text{De} = 5$

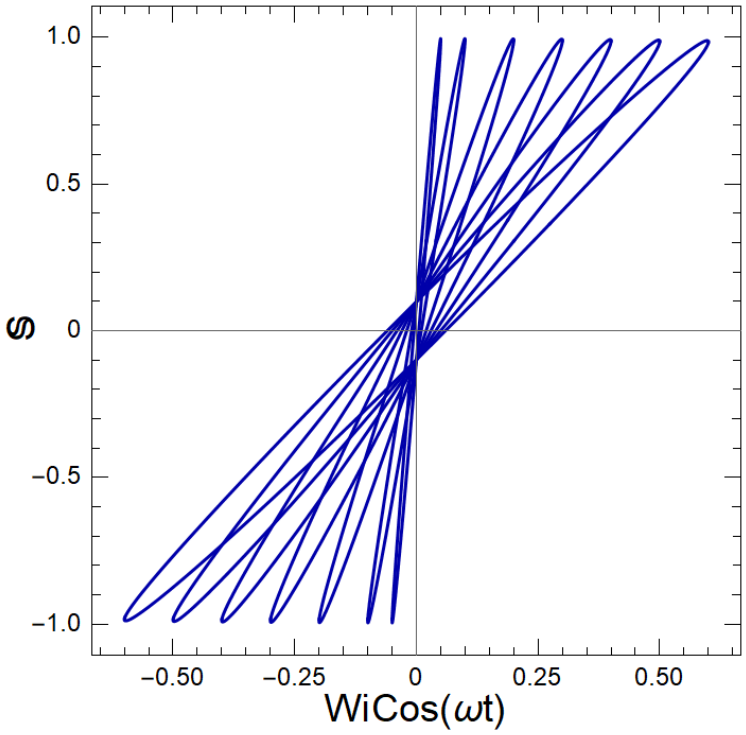

Figure 36: Dimensionless shear stress verses dimensionless shear rate. Where $\frac{\mathrm{Wi}}{\mathrm{De}} = (0.5, 1, 2, 3, 4, 5, 6)$ and $\mathrm{De} = 0.1$

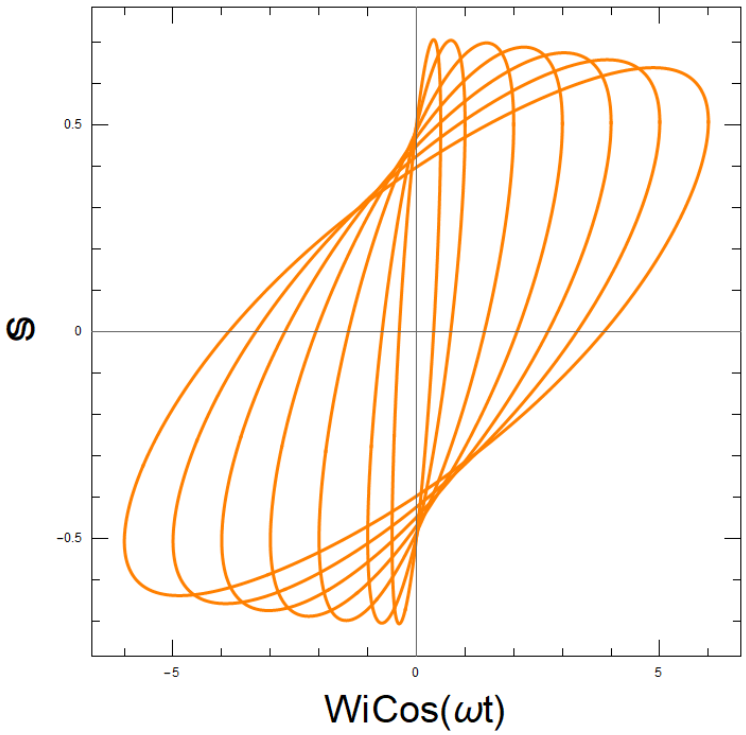

Figure 37: Dimensionless shear stress verses dimensionless shear rate. Where $\frac{\mathrm{Wi}}{\mathrm{De}} = (0.5, 1, 2, 3, 4, 5, 6)$ and $\mathrm{De} = 1$

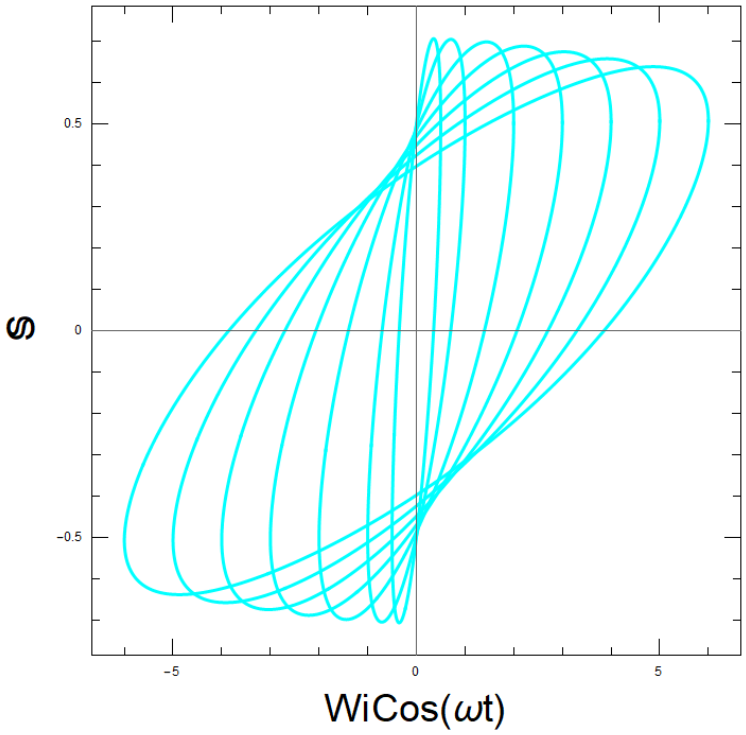

Figure 38: Dimensionless shear stress verses dimensionless shear rate. Where $\frac{\text{Wi}}{\text{De}} = (0.5, 1, 2, 3, 4, 5, 6)$ and $\text{De} = 5$

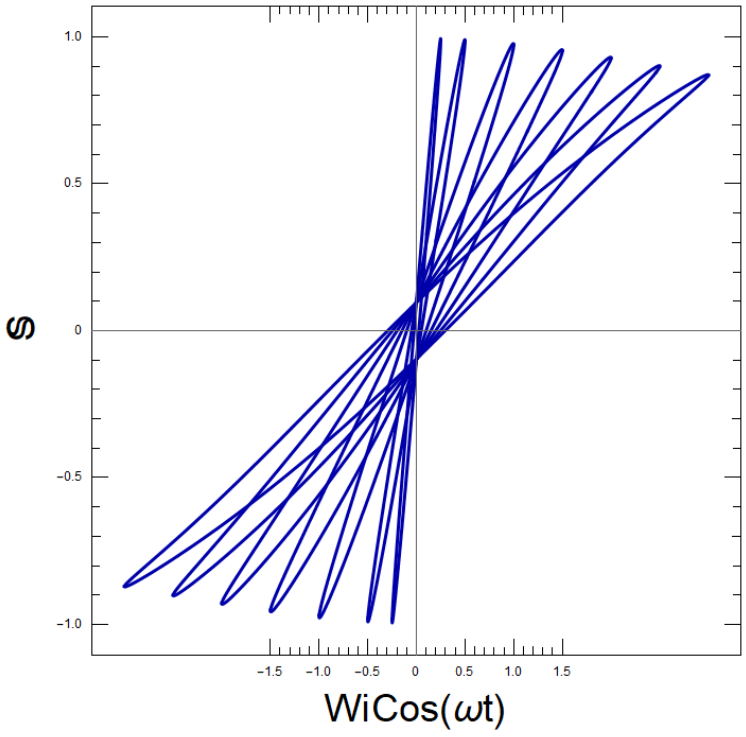

Figure 39: Dimensionless shear stress verses dimensionless shear rate. Where $\frac{\text{Wi}}{\text{De}} = (2.5, 5, 10, 15, 20, 25, 30)$ and $\text{De} = 0.1$

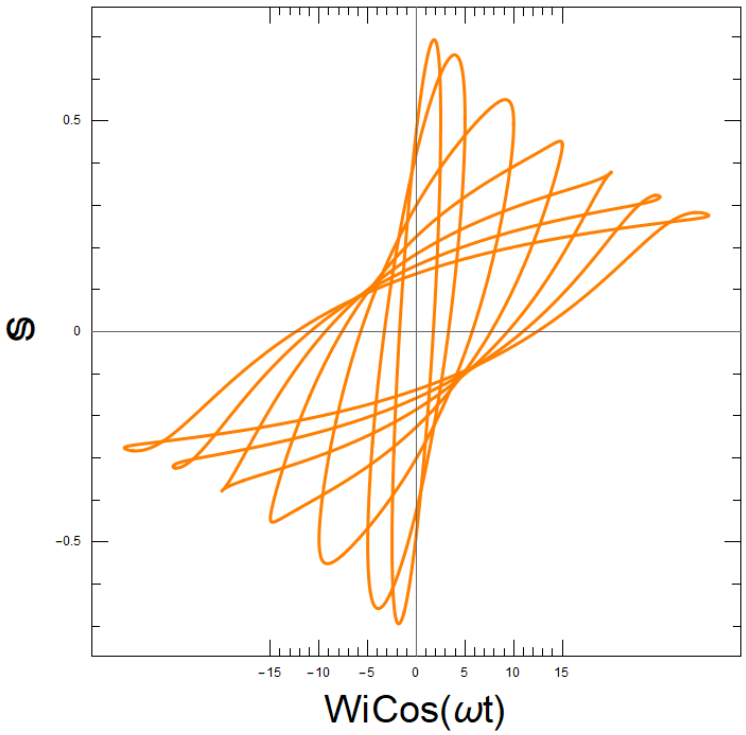

Figure 40: Dimensionless shear stress verses dimensionless shear rate. Where $\frac{\mathrm{Wi}}{\mathrm{De}} = (2.5, 5, 10, 15, 20, 25, 30)$ and $\mathrm{De} = 1$

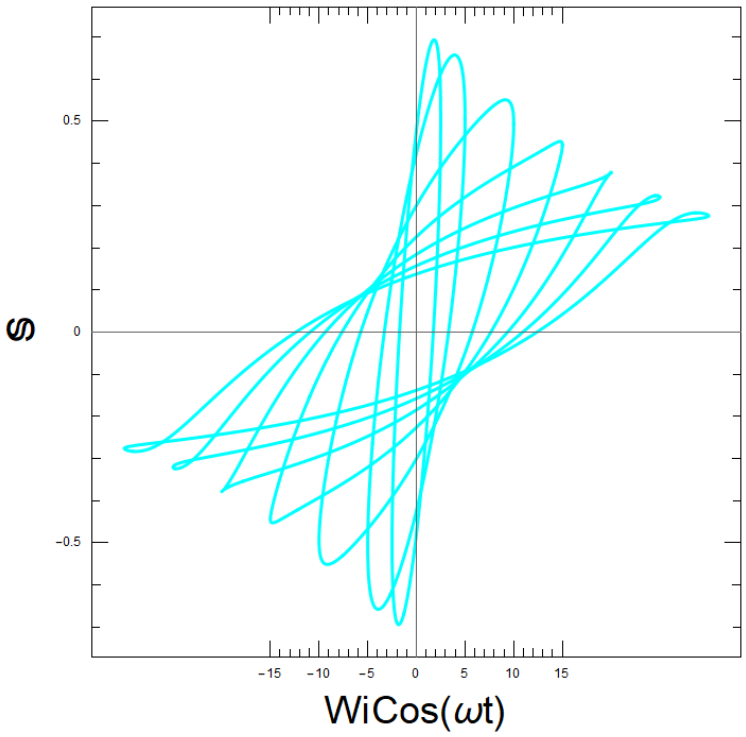

Figure 41: Dimensionless shear stress verses dimensionless shear rate. Where $\frac{\mathrm{Wi}}{\mathrm{De}} = (2.5, 5, 10, 15, 20, 25, 30)$ and $\mathrm{De} = 5$

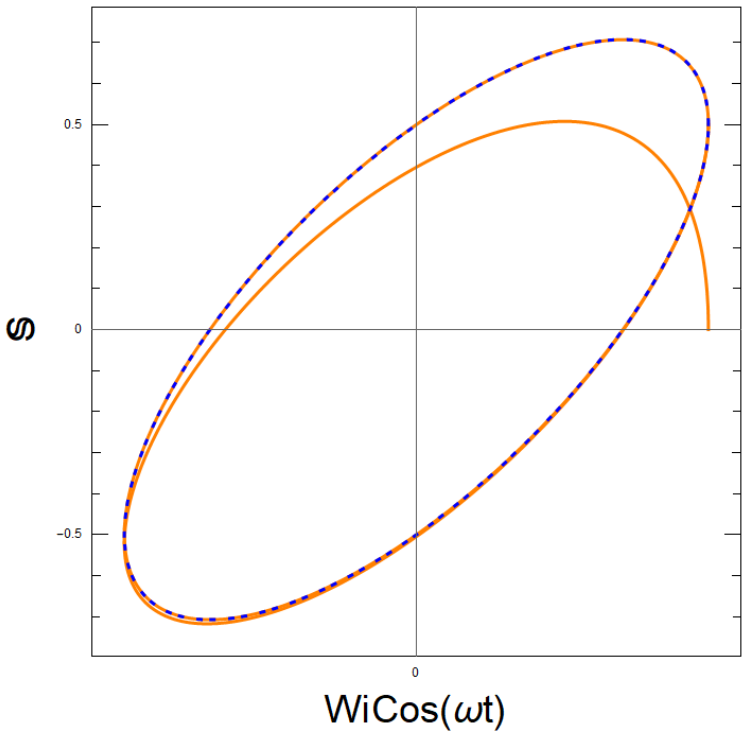

Figure 42: Start-up of linear LAOS module at De = 1 and Wi = 0.1 compared with SAOS (blue)

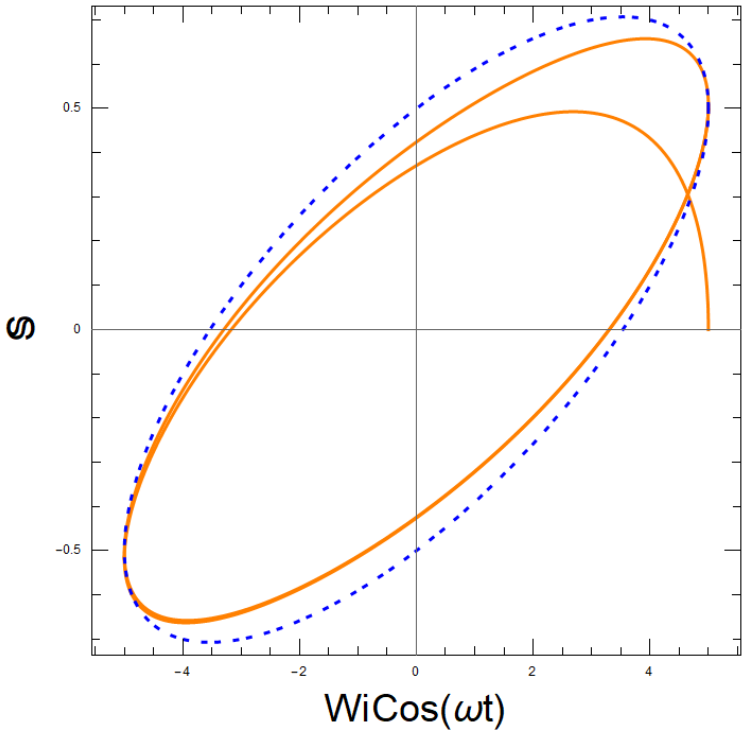

Figure 43: Start-up of linear LAOS module at De = 1 and Wi = 5 compared with SAOS (blue)

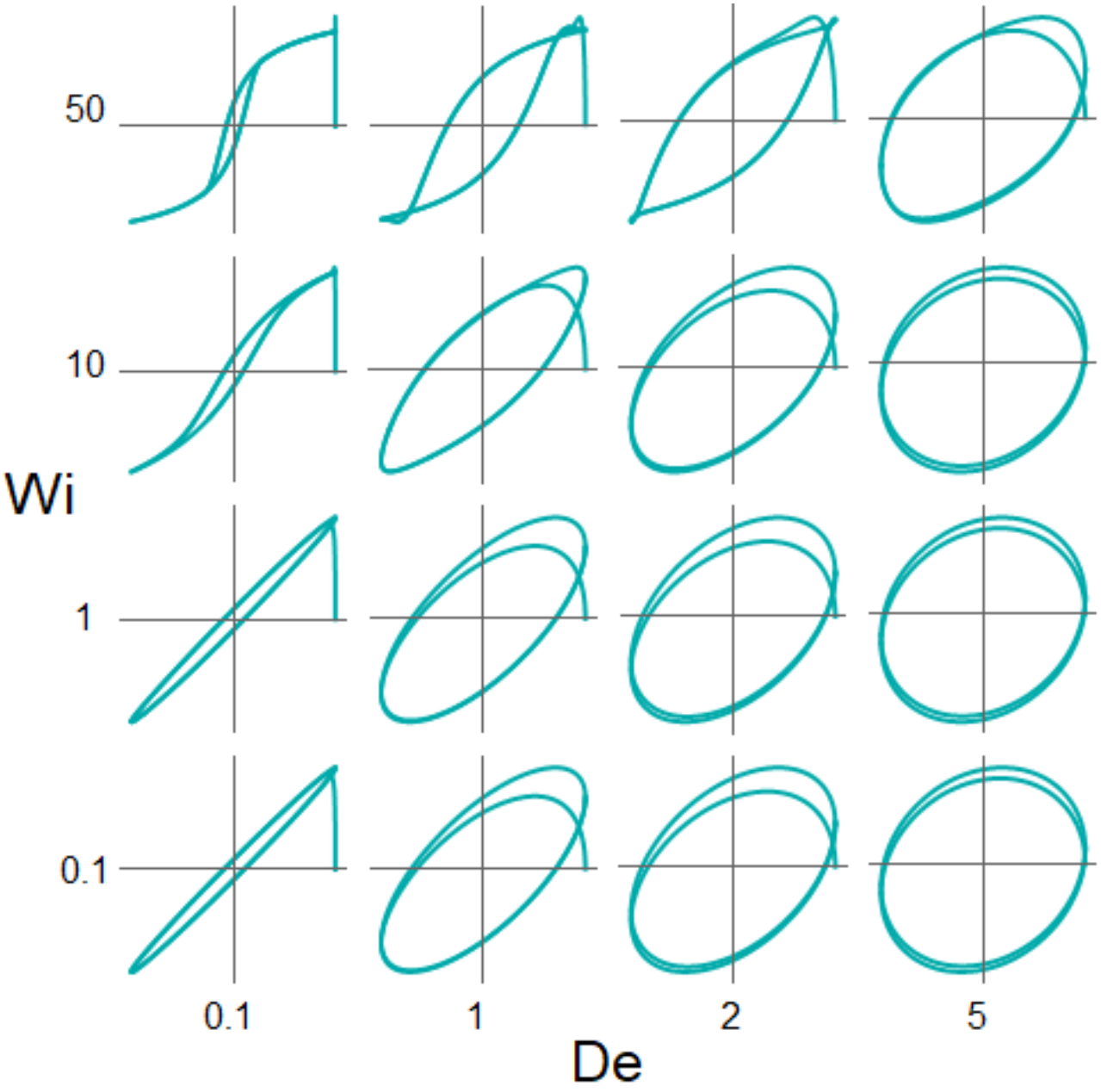

Figure 44: 4×4 Ewoldt grids of the linear LAOS module for $\mathrm{Wi} = 0.1, 1, 10, 50.$ verses $\mathrm{De} = 0.1, 1, 2, 5.$ Loops of dimensionless shear stress $\mathbb{S}$ verses $\cos \omega \mathrm{t}$

Advance modelling for exponential large amplitude oscillation shear (LAOS) model using Mathematica

With the aid of Mathematica and equation [5.31] the following figures are produced for the exponential LAOS module. The figures are grouped into constant De numbers and varying Wi numbers. The values of De numbers are 0.1,1 and 5.

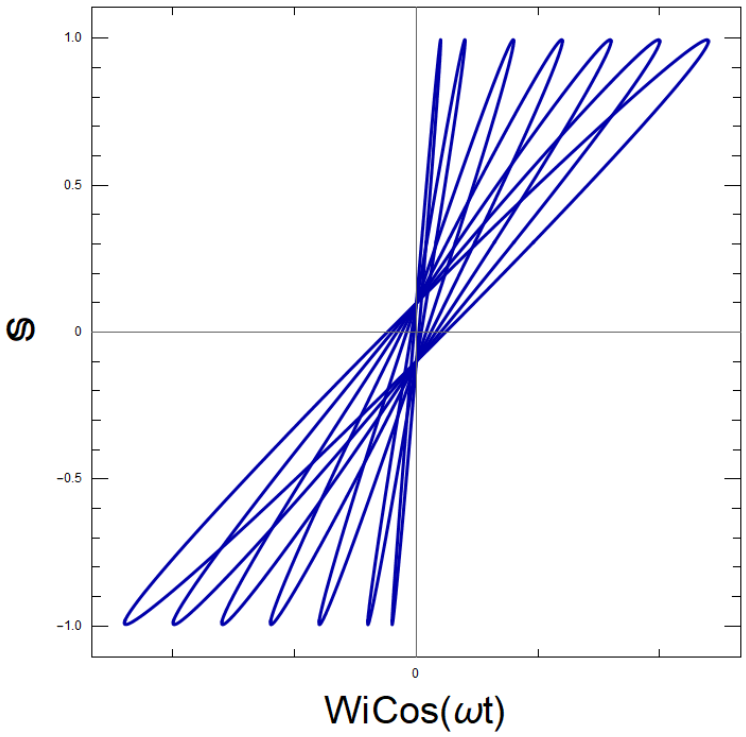

Figure 45: Dimensionless shear stress verses dimensionless shear rate. Where $\frac{\text{Wi}}{\text{De}} = (0.1, 0.2, 0.4, 0.6, 0.8, 1, 1.2)$ and $\text{De} = 0.1$

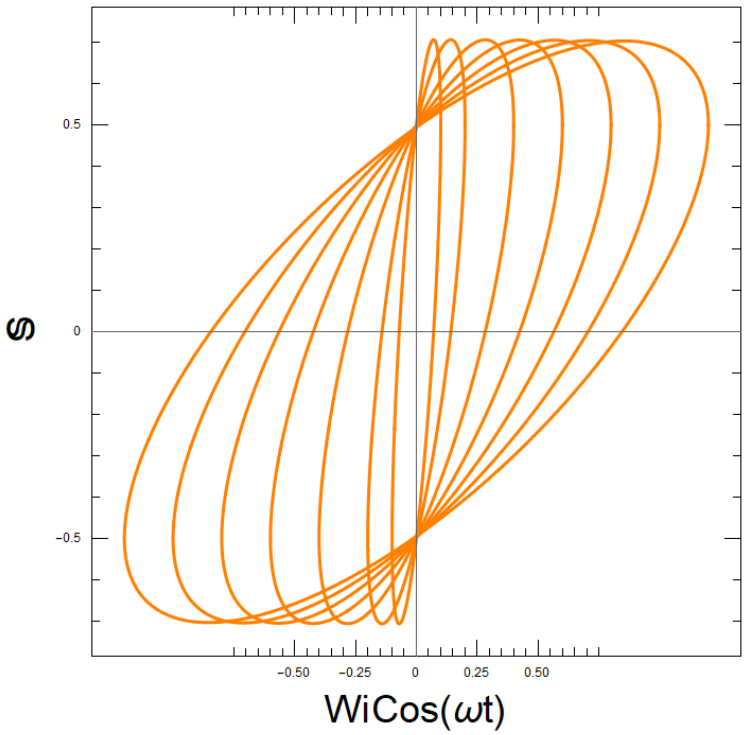

Figure 46: Dimensionless shear stress verses dimensionless shear rate. Where $\frac{\text{Wi}}{\text{De}} = (0.1, 0.2, 0.4, 0.6, 0.8, 1, 1.2)$ and $\text{De} = 1$

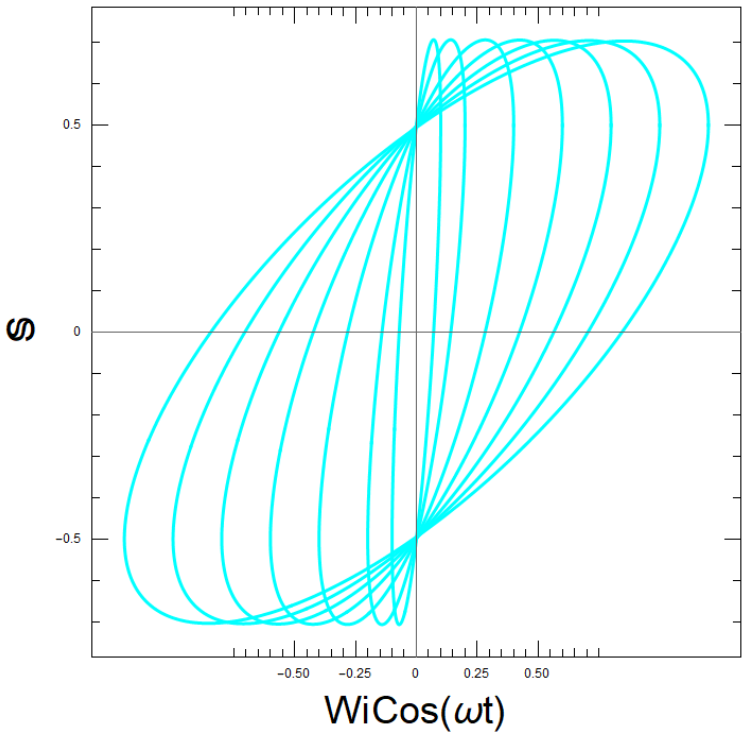

Figure 47: Dimensionless shear stress verses dimensionless shear rate. Where $\frac{\text{Wi}}{\text{De}} = (0.1, 0.2, 0.4, 0.6, 0.8, 1, 1.2)$ and $\text{De} = 5$

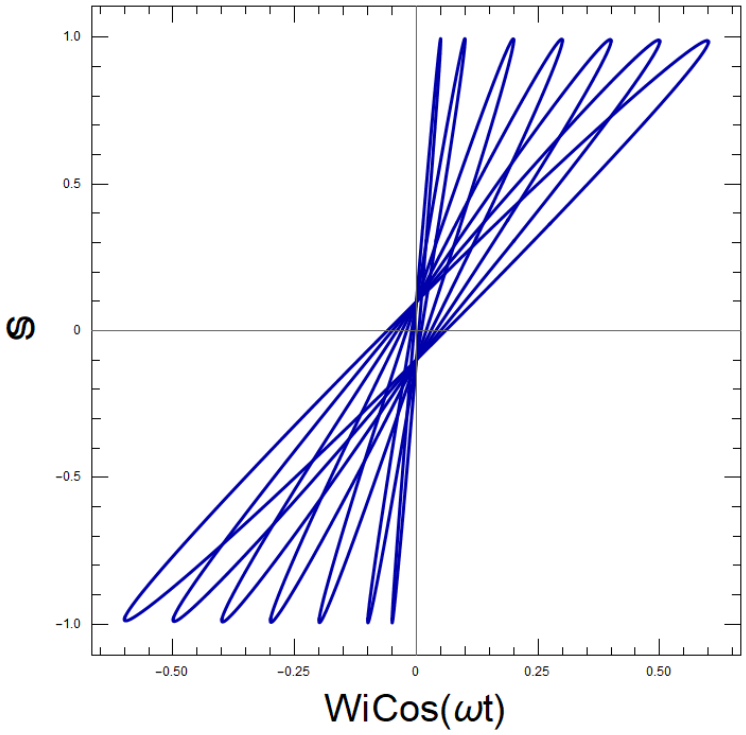

Figure 48: Dimensionless shear stress verses dimensionless shear rate. Where $\frac{\mathrm{Wi}}{\mathrm{De}} = (0.5, 1, 2, 3, 4, 5, 6)$ and $\mathrm{De} = 0.1$

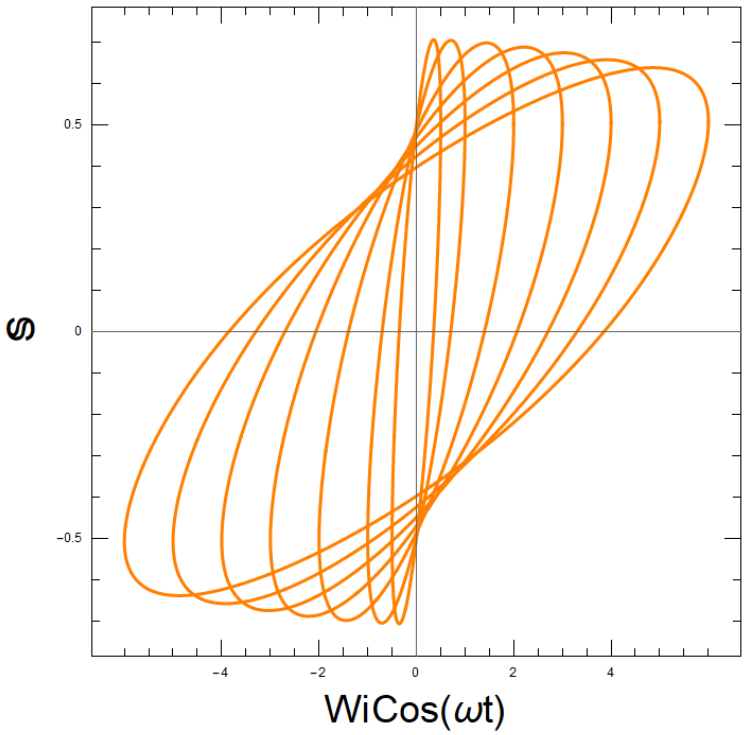

Figure 49: Dimensionless shear stress verses dimensionless shear rate. Where $\frac{\mathrm{Wi}}{\mathrm{De}} = (0.5, 1, 2, 3, 4, 5, 6)$ and $\mathrm{De} = 1$

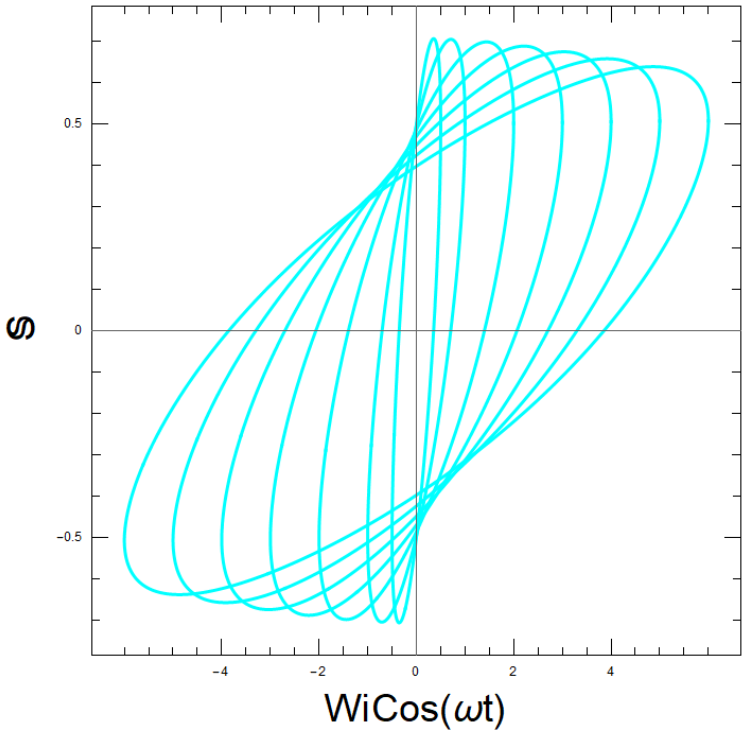

Figure 50: Dimensionless shear stress verses dimensionless shear rate. Where $\frac{\mathrm{Wi}}{\mathrm{De}} = (0.5, 1, 2, 3, 4, 5, 6)$ and $\mathrm{De} = 5$

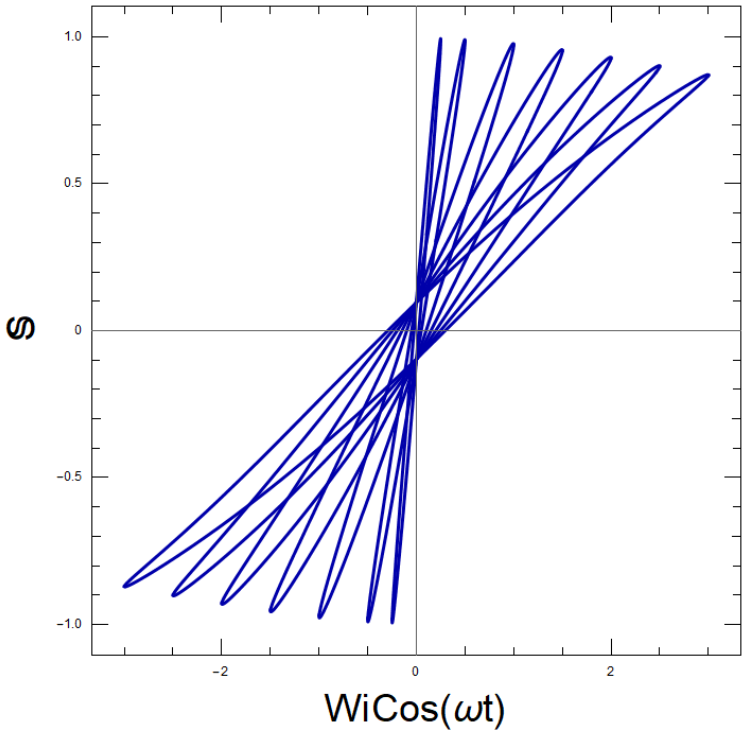

Figure 51: Dimensionless shear stress verses dimensionless shear rate. Where $\frac{\mathrm{Wi}}{\mathrm{De}} = (2.5, 5, 10, 15, 20, 25, 30)$ and $\mathrm{De} = 0.1$

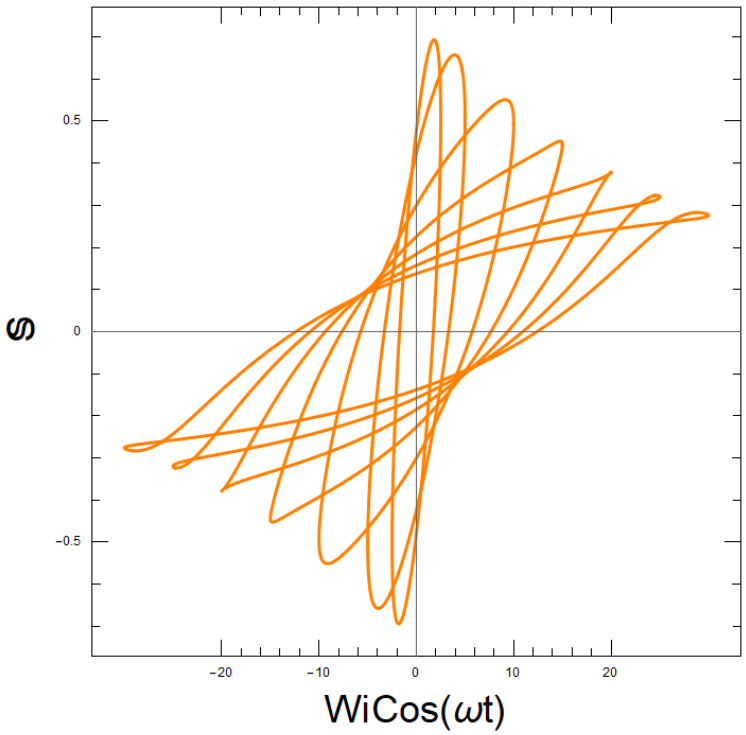

Figure 52: Dimensionless shear stress verses dimensionless shear rate. Where $\frac{\mathrm{Wi}}{\mathrm{De}} = (2.5, 5, 10, 15, 20, 25, 30)$ and $\mathrm{De} = 1$

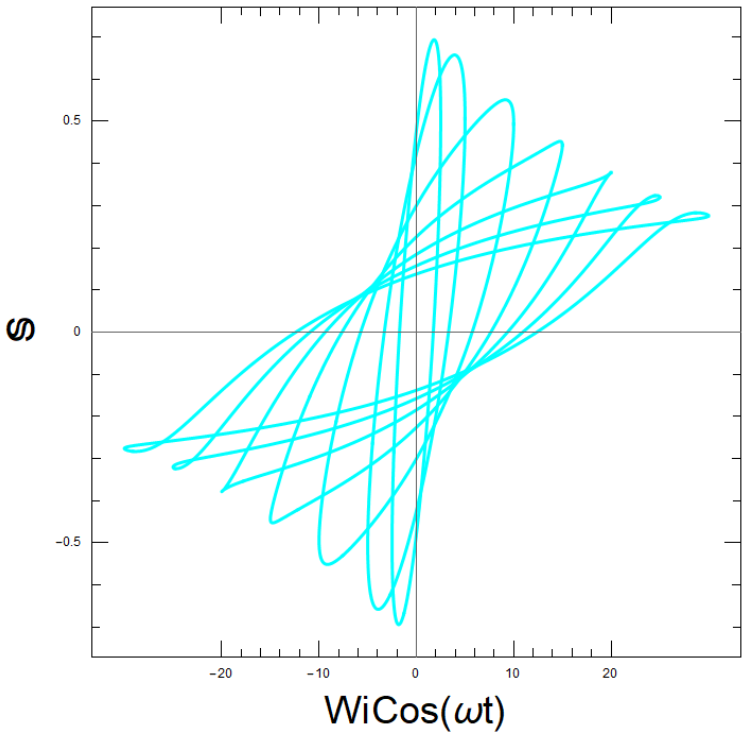

Figure 53: Dimensionless shear stress verses dimensionless shear rate. Where $\frac{\mathrm{Wi}}{\mathrm{De}} = (2.5, 5, 10, 15, 20, 25, 30)$ and $\mathrm{De} = 5$

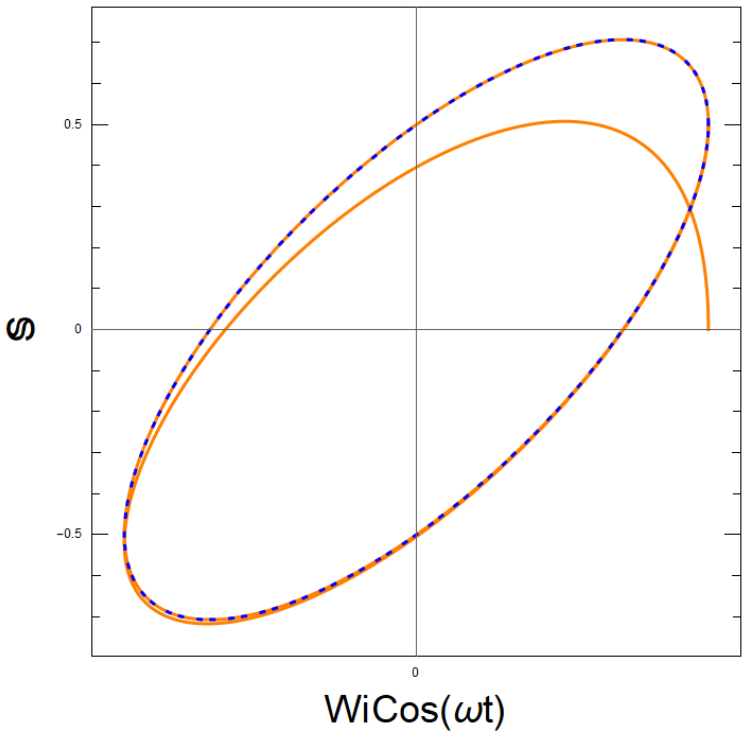

Figure 54: Start-up of exponential LAOS module at De = 1 and Wi = 0.1 compared with SAOS (blue)

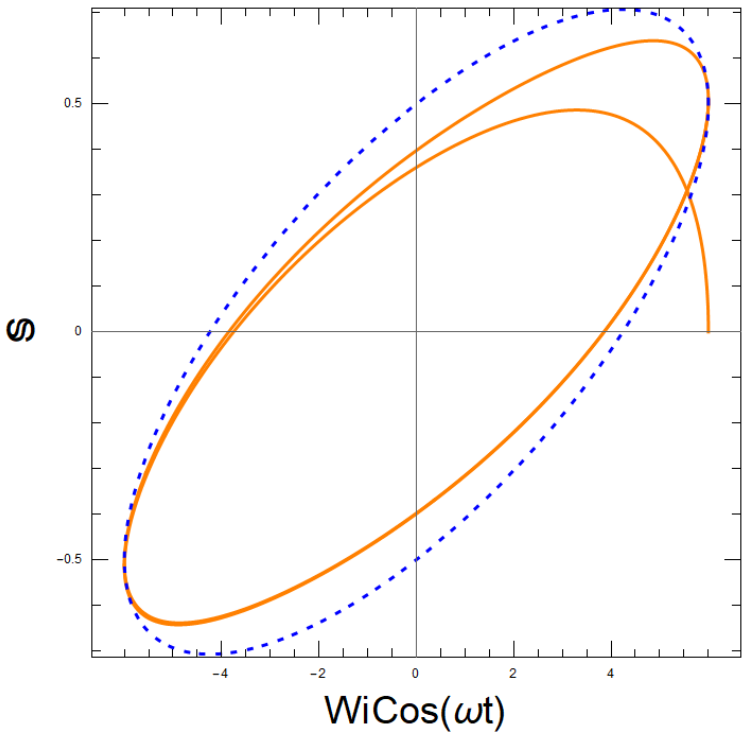

Figure 55: Start-up of exponential LAOS module at De = 1 and Wi = 5 compared with SAOS (blue)

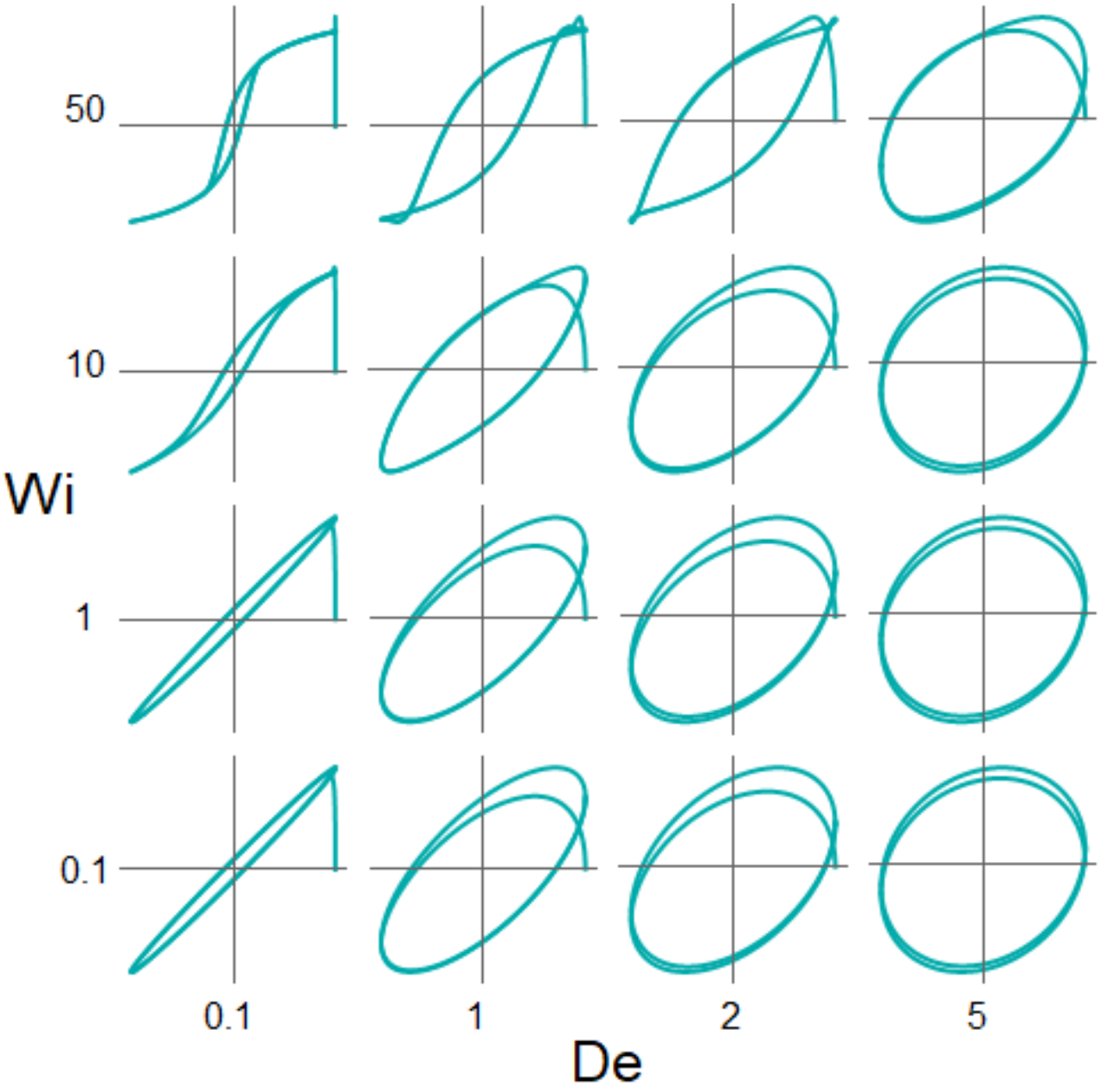

Figure 56: 4×4 Ewoldt grids of the exponential LAOS module for $\mathrm{Wi} = 0.1, 1, 10, 50$. verses $\mathrm{De} = 0.1, 1, 2, 5$. Loops of dimensionless shear stress $\mathbb{S}$ verses $\cos \omega t$

Conclusions

The purpose of this piece was to probe into the behaviour of material functions of non-Newtonian fluids analytically, especially at inception and cessation of steady shear flow. With a lot of research already in this field the main focus was to study the anticipated results of polymeric fluids under certain defined parameters using advanced modelling techniques.

It is seen that the growth functions for viscosity and normal stress for the Phan-Thien-Tanner modules (linear and exponential) are higher at low Weissenberg (Wi) numbers and as the (Wi) increases viscosity and normal stress growth diminishes.

The higher the (Wi) numbers the lower the rate of viscosity and stress growth. The behaviour of the viscosity growth function and normal stress coefficient at start-up of steady flow is also confirmed where there is an overshoot at higher (Wi) numbers but diminishes as Wi decreases and approaches 1 at different (Wi) numbers.

The function is oscillatory but is only the first oscillation which is clearly seen while the subsequent ones are not visible in the plots and the flow stabilizes faster at higher Wi numbers. Comparing the normalised viscosity to the first normal stress coefficient it is noticed that the growth in the former is faster than in the later.

At cessation, the normalized viscosity and stress coefficient functions approaches zero; where the rate is faster at high Wi numbers.

With respect to the large amplitude oscillation shear, the behaviour of the steady flow is also analyzed for the linear and exponential modules. The start up is omitted for better visuals. The shear stress as a function of shear rate diminishes with increasing Wi numbers. It is more consistent at lower De values but varies as the De increases. At very high Wi numbers there is a dramatic shift from the normal cone-plate form to an overlapping one. The flow when Wi $<$ Wi tends to signify small amplitude oscillation shear whiles the Wi $>$ Wi signifies LAOS.

The results from these modules for initiation and cessation can be used in both industrial and experimental fields of endeavour. The pattern of the modules can help predict the viscosity and shear stress behaviour at inception ,cessation and understand the time limits involved polymer degradation and increase in mobility ratio.

The knowledge here is also vital in all polymer applications and manufacturing.

References

[] *Enhance oil recovery methods*. https://www.npd.no/en/facts/publications/reports2/resource-report/. Accessed: 2020-07-14.

[] *Power-law graph*. https://http://www.rheologyschool.com/advice/rheology-tips/35-making-use-of-models-the-power-law-or-ostwald-model. Accessed: 2020-06-19.

[] *The Many applications of polymers*. https://www.gellnerindustrial.com/applications-polymers/. Accessed: 2020-03-26.

[] *Wolfram Mathematica*. https://en.wikipedia.org/wiki/Wolfram_Mathematica/ https://www.wolfram.com/mathematica/?source=nav. Accessed: 2020-05-19.

[AAG14] M Algharaib, A Alajmi, and R Gharbi. "Improving polymer flood performance in high salinity reservoirs". In: *Journal of Petroleum Science and Engineering* 115 (2014), pp. 17–23.

[BAH87] Robert Byron Bird, Robert C Armstrong, and Ole Hassager. "Dynamics of polymeric liquids. Vol. 1: Fluid mechanics". In: (1987).

[BG16] R Byron Bird and A Jeffrey Giacomin. "Polymer fluid dynamics: Continuum and molecular approaches". In: *Annual review of chemical and biomolecular engineering* 7 (2016), pp. 479–507.

[Fer+19] LL Ferrás et al. "A generalised Phan–Thien—Tanner model". In: *Journal of Non-Newtonian Fluid Mechanics* 269 (2019), pp. 88–99.

[GK12] VB Gupta and VK Kothari. *Manufactured fibre technology*. Springer Science & Business Media, 2012.

[Hyu+11] Kyu Hyun et al. "A review of nonlinear oscillatory shear tests: Analysis and application of large amplitude oscillatory shear (LAOS)". In: *Progress in Polymer Science* 36.12 (2011), pp. 1697–1753.

[Jin04] NIU Jin-gang. "Practices and understanding of polymer flooding enhanced oil recovery technique in Daqing oilfield [J]". In: *Petroleum Geology & Oilfield Development in Daqing* 5 (2004), p. 024.

[Ner14] Roy Nersesian. *Energy for the 21st century: a comprehensive guide to conventional and alternative sources*. Routledge, 2014.

[Poo12] RJ Poole. "The deborah and weissenberg numbers". In: *Rheol. Bull* 53.2 (2012), pp. 32–39.

[Pou+19] P Poungthong et al. "Power series for normal stress differences of polymeric liquids in large-amplitude oscillatory shear flow". In: *Physics of Fluids* 31.3 (2019), p. 033101.

[Ram19] Mark S Ramsey. *Practical Wellbore Hydraulics and Hole Cleaning: Unlock Faster, More Efficient, and Trouble-free Drilling Operations*. Gulf Professional Publishing, 2019.

[Ret78] Oil Shale Retorting. "Effects of Particle Size and Heating Rate on Oil Evolution and Intraparticle Oil Degradation; Campbell et al". In: *Situ* 2.1 (1978), pp. 1–47.

[SA19] Dmitry Shogin and Per Amund Amundsen. "The Charged FENE-P Dumbbell model: explaining the rheology of dilute polyelectrolyte solutions". In: *arXiv preprint arXiv:1907.00003* (2019).

[SGK15] Chaimongkol Saengow, Alan Jeffrey Giacomin, and Chanyut Kolitawong. "Exact Analytical Solution for Large-Amplitude Oscillatory Shear Flow". In: *Macromolecular Theory and Simulations* 24.4 (2015), pp. 352–392.

[Sho20] Dmitry Shogin. "Start-up and cessation of steady shear and extensional flows: Exact analytical solutions for the affine linear Phan-Thien-Tanner fluid model". In: *arXiv preprint arXiv:2006.04116* (2020).

[TA19] M Toorani and M Aliofkhazraei. "Review of electrochemical properties of hybrid coating systems on Mg with plasma electrolytic oxidation process as pretreatment". In: *Surfaces and Interfaces* 14 (2019), pp. 262–295.

[TT77] Nhan Phan Thien and Roger I Tanner. "A new constitutive equation derived from network theory". In: *Journal of Non-Newtonian Fluid Mechanics* 2.4 (1977), pp. 353–365.

[VJA15] Luis E Valencia, Lesley A James, and Karem Azmy. "Pore System Changes During Experimental Polymer Flooding in Ben Nevis Formation Sandstones, Hebron Field, Offshore Eastern Canada". In: *International Conference & Exhibition*. 2015.

[YL11] Robert J Young and Peter A Lovell. *Introduction to polymers*. CRC press, 2011.